Hindawi Publishing Corporation
EURASIP Journal on Advances in Signal Processing
Volume 2008, Article ID 439523, 16 pages
doi:10.1155/2008/439523

Research Article

Comparison of Semidistributed Multinode TOA-DOA Fusion Localization and GPS-Aided TOA (DOA) Fusion Localization for MANETs

Zhonghai Wang and Seyed Zekavat

Department of Electrical and Computer Engineering, College of Engineering, Michigan Technological University, Houghton, MI 49931, USA

Correspondence should be addressed to Zhonghai Wang, wzhongha@mtu.edu

Received 20 February 2008; Revised 30 July 2008; Accepted 6 October 2008

Recommended by Fredrik Gustafsson

This paper evaluates the performance of a semidistributed multinode time-of-arrival (TOA) and direction-of-arrival (DOA) fusion localization technique in terms of localization circular error probability (CEP). The localization technique is applicable in mobile ad hoc networks (MANETs) when global positioning system (GPS) is not available (GPS denied environments). The localization CEP of the technique is derived theoretically and verified via simulations. In addition, we theoretically derive the localization CEP of GPS-aided TOA fusion and GPS-aided DOA fusion techniques, which are also applicable in MANETs. Finally, we compare these three localization techniques theoretically and via simulations. The comparison confirms that in moderate scale MANETs, the multinode TOA-DOA fusion localization technique achieves the best performance; while in large scale MANETs, GPS-aided TOA fusion leads to the best performance.

1. INTRODUCTION

Node localization is required in ad hoc networks to support resource allocation [1], routing [2, 3], situation awareness [4, 5], and so forth. Many coarse and fine localization techniques applicable in ad hoc networks have been introduced in the literature. Coarse localization techniques that depend on power measurement include node connectivity fusion [6–8], and received signal strength indication (RSSI) [9, 10]. The proposed techniques in [6, 7] assume static base-nodes, while the approach proposed in [8] considers node mobility. Fine localization techniques that depend on TOA and/or DOA estimation include fusion of GPS (global positioning system) and communication [11, 12], time-of-arrival (TOA) or time-difference-of-arrival (TDOA) fusion [13–16], direction-of-arrival (DOA) fusion [17–19], TOA-DOA joint estimation [20], centralized multinode TOA-DOA fusion [21], and hybrid positioning techniques [22–24]. Please note that when constraint is available, such as geometric constraint [19], a part of errors (especially those large errors) are detected and removed in data processing; hence, higher performance could be achieved.

In this paper, we define base-nodes as nodes capable of TOA and/or DOA estimation. In other words, base-nodes are capable of estimating the position of other nodes located in their coverage area. In addition, target-nodes are those nodes whose positions are estimated by the base-nodes.

In mobile ad hoc networks (MANETs), all nodes are moving. Accordingly, the environment and the position of base-nodes are changing. As a result, techniques such as node connectivity fusion and RSSI that require fixed base-nodes' position and fixed environment are not applicable. In these situations, if GPS can be used to determine base-nodes' position, the techniques requiring known base-nodes' position are capable of positioning. Examples are fusion of GPS and communication, GPS-aided TOA fusion [25], and GPS-aided DOA fusion [26]. In many applications, GPS signal is not available. In this case, techniques that function independent of GPS should be implemented. Examples of GPS-independent localization techniques are TOA-DOA

joint estimation, centralized and semidistributed multinode TOA-DOA fusion localization schemes. The proposed semidistributed approach is opposed to the centralized scheme. In the centralized scheme, only one base-node is in charge of data processing (fusion) to localize all target-nodes. Thus, that base-node needs a very high processing power. In the proposed semidistributed scheme, taking into account the geometrical distribution, each base-node undertakes the data processing (fusion) to localize some target-nodes (so it is called "semi") in its coverage area. Here, the processing power would be distributed across base-nodes. Thus, the processing power assigned to each base-node would be lower.

The centralized and semidistributed multinode TOA-DOA fusion localization techniques take the advantage of base-nodes' property, capable of estimating other nodes position independently. The reference and nonreference base-nodes localize each other and fuse the localization information to improve base-nodes' position estimation accuracy. Then, they cooperate to estimate target-nodes' position. The target-nodes' position is achieved via data fusion across multiple base-nodes.

In centralized multinode TOA-DOA fusion, the data processing is entirely accomplished in the reference base-node; while in the semidistributed fusion technique, the data processing is distributed across multiple base-nodes. In addition, in the semidistributed scheme, the reference base-node is selected via a suboptimal method that minimizes the average positioning error. If the two localization methods apply the same reference base-node selection scheme, their localization accuracy would be equal.

TOA fusion and TDOA fusion performance is the same [27]; hence, we only consider the performance of GPS-aided TOA fusion. In GPS-aided TOA (DOA) fusion scheme, GPS receivers are applied to estimate base-nodes' position. Then target-node's TOAs (DOAs) estimated by multiple base-nodes, and, base-nodes' positions are fused to estimate the target-node position. In these techniques, GPS positioning error can be transformed to TOA (DOA) estimation error, and it equivalently increases the target-node positioning error. The TOA estimation error generated by GPS positioning error is independent of the distance between target node and base-node; but the DOA estimation error generated by GPS positioning error is a function of the distance between target-node and base-node. If target-node is far from base-node, the DOA estimation error generated by GPS positioning error is negligible. However, if target-node is close to base-node, the DOA estimation error generated by GPS positioning error is considerable.

In semidistributed multinode TOA-DOA fusion localization, TOA and DOA are estimated at base-nodes by processing signals transmitted by base-nodes or target-nodes. If line-of-sight (LOS) is available, then a good performance can be achieved. In GPS-aided TOA (DOA) fusion, GPS positioning information and target-node TOA (DOA) information must be computed at base-nodes. The sources of positioning error in these systems include the lack of availability of the LOS between the transmitter and the receiver as well as reflection effects (e.g., in the downtown areas) that reduces the positioning accuracy of the GPS.

In the proposed semidistributed technique and GPS-aided DOA fusion, major errors (a complete confusion) may occur if the LOS signal between the base-nodes and target-nodes is blocked. GPS-aided TOA (DOA) fusion requires LOS to both GPS satellites and target-node; while the semidistributed method needs LOS between base-nodes and base-nodes to target-node. Hence, when signals to GPS satellites are blocked, the semidistributed multinode TOA-DOA fusion may perform.

Because nodes are moving, the base-nodes positions and target-nodes TOA and/or DOA used in the fusion to localize target-nodes are not computed simultaneously. Here, we assumed a similar system as the wireless local positioning system (WLPS) discussed in [20]. WLPS enables a base-node to localize target-nodes periodically: the base-nodes transmit periodic signals with a period that is called identification request repetition time (IRT) and target-nodes automatically respond to those signals. One IRT is assigned to estimate base-nodes position and another IRT is assigned to estimate target-nodes TOA and DOA; hence, the time difference between base-node position estimation and target-nodes TOA and DOA estimation is about IRT. Assuming IRT = 24 milliseconds, a node with a speed of 10 m/s (outdoor) would move 0.24 meters within this time period. This error is generated by nodes movement and would be tolerable in outdoor application.

GPS positioning updating rate is limited to 20 Hz. This limits the GPS-based positioning updating rate. Higher updating rate would involve with some error, if the nodes mobility increases. If the system positioning updating rate is 20 Hz and base-nodes TOA/DOA estimation are synchronized with GPS, then there would be no time difference between the base-node position estimation and target-nodes TOA (DOA) estimation. This removes the latency across these two estimations and reduces their associated errors. In this work, we assume full synchronization.

Different localization performance evaluation standards have been introduced. These standards include cumulative localization error distribution [6], mean and standard deviation of the positioning error [9], normalized mean square of the positioning error [21], and geometrical dilution of precision (GDOP) [14, 28, 29]. GDOP only provides the positioning performance of a system considering single category of measurement (TOA or DOA) and assuming the measurement errors are independent and identically distributed. Normalized mean square, mean and standard deviation of the positioning error can be applied to any positioning system, but it only provides one statistics of the positioning performance. Cumulative localization error distribution, also known as circular error probability (CEP) [30], incorporates the cumulative density function (CDF) of the positioning error. Hence, it includes more information on the statistics of the positioning error. In addition, it can be applied to any positioning system in any scenario. Accordingly, in this paper, we evaluate the performance of the semidistributed multinode TOA-DOA fusion localization technique in terms of localization CEP in the condition of all target-nodes being localized; then, we compare it to that of GPS-aided TOA (DOA) fusion. In the condition of not

all target-nodes being localized, we use the probability of target-nodes being localized as standard to compare the three localization methods.

The rest of the paper is organized as follows. Section 2 reviews the semidistributed multinode TOA-DOA fusion localization scheme. Section 3 derives the localization CEP of the semidistributed multinode TOA-DOA fusion. Section 4 studies the impact of GPS positioning error on TOA (DOA) estimation and derives the localization CEP of these two methods. Section 5 presents simulation results, comparison of the introduced techniques and discussions. Section 6 concludes the paper.

2. SEMIDISTRIBUTED MULTINODE TOA-DOA FUSION LOCALIZATION TECHNIQUE

Here, we briefly review the semidistributed multinode TOA-DOA fusion localization technique.

2.1. MANET structure and assumptions

Here, we assume the MANET that apply semidistributed multinode TOA-DOA fusion localization are composed of two categories nodes: (i) base-nodes equipped with antenna arrays that are capable of estimating the TOA and DOA of target-nodes or other base-nodes; and, (ii) target-nodes equipped with omnidirectional antennas that respond to the inquiring signal transmitted by base-nodes. Here, base-nodes transmit a signal periodically that requests all target-nodes in its coverage area to announce their availability by sending a signal back to the base-node automatically. The base-node calculates the TOA of the received signal compared to the transmitted one in order to calculate the range (see [20]).

Thus, base-nodes and target-nodes communicate. This communication can be incorporated to transmit other information. For example, if some sensors are installed at target-nodes, the corresponding information can be communicated with base-nodes and vice versa. Hence, the proposed system may also support the process of communication within an ad hoc sensor network.

In addition, antenna arrays installed at the receiver of base-nodes estimate the DOA. Combining DOA and TOA, each base-node would be able to localize the target-nodes in its coverage area independently. Different TOA and DOA estimation techniques and their corresponding error analysis for antenna arrays have been discussed in [31–33]. Direct sequence code division multiple access (DS-CDMA) is applied to maintain orthogonality across the signals transmitted by each node and to improve the performance.

The MANET structure is shown in Figure 1. Here, we assume that the following hold. (1) There are n base-nodes and m target-nodes (usually $n \ll m$) in the MANET (to compare multinode TOA-DOA fusion localization technique with GPS-aided TOA (DOA) fusion, we set $n \geq 3$). (2) All nodes in the system are uniformly distributed in the MANET. (3) Every base-node localizes target-nodes located in its coverage area (radius is $R_{\max}$), and the MANET coverage radius is $\alpha R_{\max}$. The multinode TOA-DOA fusion

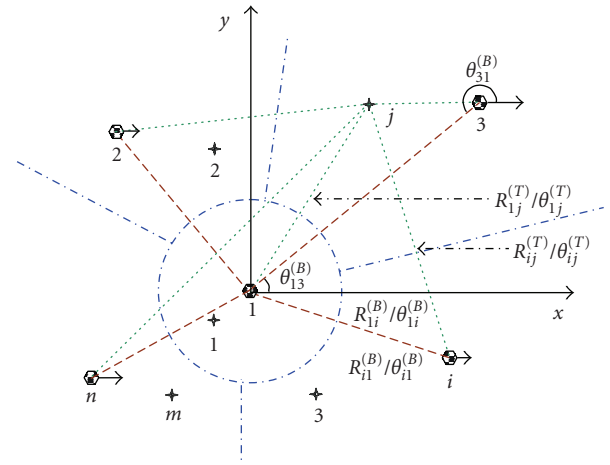

Figure 1: The structure of the MANET that applies semidistributed multinode TOA-DOA fusion.

and its localization CEP are derived in the condition of $0 < \alpha \leq 0.5$ (i.e., all base-nodes localize all target-nodes in the MANET). A simple geometry can justify that if the MANET coverage area radius is more than $0.5R_{\max}$, some base-nodes might not be able to localize all target-nodes in the MANET. The short coming of the semidistributed multinode TOA-DOA fusion in the condition of $0.5 < \alpha$ is discussed in Section 2.4. (4) One base-node (e.g., base-node 1) is carefully selected as the reference base-node, whose local coordinates are considered as the main coordinates, in which all nodes are localized. (5) TOA (range) estimation errors are independent zero mean Gaussian random variables with the same variance σ_{TOA}^2 (σ_R^2), and DOA estimation errors are also independent zero mean Gaussian random variables with the same variance σ_θ^2. (6) Both range and angle estimation errors are small (when we calculate the positioning error using linearization technique, higher order terms can be ignored); (7) DOA angle is measured anticlockwise with respect to the x-axis (e.g., east); and, (8) all base-nodes simultaneously localize target-nodes.

2.2. Localization scheme

The localization scheme includes three main stages.

(1) *The reference base-node selection and cluster formation:* a base-node is selected as the reference base-node to achieve optimal performance, and all nodes are localized in the reference base-node's coordinate. A suboptimal scheme is used to select the reference base-node to decrease the computational and time costs (see Appendix A). Clusters are formed to enhance the positioning updating rate. Each cluster consists of one base-node and multiple target-nodes. The base-node is in charge of target-nodes' position estimation data fusion in that cluster. The clustering

scheme uniformly distributes all target-nodes across all clusters. Note that all nodes in the MANET are dynamic. Hence, the reference base-node selection and cluster formation would be performed periodically to maintain the positioning accuracy. Based on (11) and (12) below and the relevant explanations, the accuracy is independent of clustering. In the following discussion, we assume base-node 1 is the reference base-node.

(2) *Nonreference base-nodes position estimation:* any pair of nonreference base-node (base-node i, $i \in \{2,\ldots, n\}$) and the reference base-node (base-node 1), that is, $(i,1)$, localize each other. Then, the localization information is fused at the nonreference base-node to estimate the nonreference base-node position. Accordingly, all nonreference base-nodes would find their position with respect to the reference base-node. Then, nonreference base-nodes broadcast their position. Hence, each base-node knows all base-nodes' position.

(3) *Target-nodes position estimation:* there are four steps in this stage: (a) base-nodes find the position of target-nodes in their coverage area, for example, in Figure 1, base-nodes 1 to n localize target-nodes 1 to m. Note that in Figure 1 base-node 3 is in charge of the data fusion of target-node j, and, base-node 1 is in charge of the data fusion of target-node 1; (b) base-nodes broadcast the target-node position information; (c) only the base-node in charge of the data fusion of a target-node receives the broadcasted target-node position, for example, only base-node 3 receives the broadcasted position information of target-node j; (d) the base-node in charge of the target-node's position estimation data fusion fuses the position information of that target-node provided by multiple base-nodes to localize the target-node.

2.3. Multinode TOA-DOA fusion

Comparing to the centralized scheme, the semidistributed method improves the positioning updating rate and reduces the requirement for the reference base-node. The data fusion technique in the two methods is the same; in the semidistributed method, multiple base-nodes are in charge of data fusion; while in the centralized scheme, the data fusion is accomplished only by the reference base-node. The associated fusion equations are derived in [21]. Here, we only review the equations required in this paper.

2.3.1. Nonreference base-nodes position estimation fusion

The reference base-node (base-node 1) estimates nonreference base-node i's $(i \neq 1)$ position as $(R_{1i}^{(B)}, \theta_{1i}^{(B)})$ and nonreference base-node i estimates the reference base-node position as $(R_{i1}^{(B)}, \theta_{i1}^{(B)})$. The base-node i's position is estimated as $(\hat{R}_{1i}^{(B)}, \hat{\theta}_{1i}^{(B)})$ via fusing $(R_{1i}^{(B)}, \theta_{1i}^{(B)})$ and $(R_{i1}^{(B)}, \theta_{i1}^{(B)})$ using weighted sum. The fusion objective function is the minimization of the mean square of the base-node i's positioning circular error, which is the distance between the real node position and the estimated one. By minimizing the mean square of the positioning circular error, the fused base-node i's position in the main polar coordinates is calculated [21]

$$\hat{R}_{1i}^{(B)} = \frac{R_{1i}^{(B)} + R_{i1}^{(B)}}{2},$$
$$\hat{\theta}_{1i}^{(B)} = \begin{cases} \dfrac{\theta_{1i}^{(B)} + \theta_{i1}^{(B)} - \pi}{2}, & \theta_{1i}^{(B)} < \pi, \\ \dfrac{\theta_{1i}^{(B)} + \theta_{i1}^{(B)} + \pi}{2}, & \theta_{1i}^{(B)} \geq \pi. \end{cases} \tag{1}$$

In the main rectangular coordinates, the base-node i's position $(x_{1i}^{(B,t)}, y_{1i}^{(B,t)})$ corresponds to

$$x_{1i}^{(B,t)} = \hat{x}_{1i}^{(B)} + \Delta\hat{x}_{1i}^{(B)} = (\hat{R}_{1i}^{(B)} + \Delta\hat{R}_{1i}^{(B)}) \cdot \cos(\hat{\theta}_{1i}^{(B)} + \Delta\hat{\theta}_{1i}^{(B)}),$$
$$y_{1i}^{(B,t)} = \hat{y}_{1i}^{(B)} + \Delta\hat{y}_{1i}^{(B)} = (\hat{R}_{1i}^{(B)} + \Delta\hat{R}_{1i}^{(B)}) \cdot \sin(\hat{\theta}_{1i}^{(B)} + \Delta\hat{\theta}_{1i}^{(B)}). \tag{2}$$

In (2), $\Delta\hat{R}_{1i}^{(B)}$ $(\Delta\hat{\theta}_{1i}^{(B)})$ is the fused range (angle) estimation error, $(\hat{x}_{1i}^{(B)}, \hat{y}_{1i}^{(B)})$ is the estimated base-node i's position by fusion. The positioning error $(\Delta\hat{x}_{1i}^{(B)}, \Delta\hat{y}_{1i}^{(B)})$ corresponds to

$$\Delta\hat{x}_{1i}^{(B)} = \Delta\hat{R}_{1i}^{(B)} \cos\hat{\theta}_{1i}^{(B)} - \Delta\hat{\theta}_{1i}^{(B)} \cdot \hat{R}_{1i}^{(B)} \sin\hat{\theta}_{1i}^{(B)},$$
$$\Delta\hat{y}_{1i}^{(B)} = \Delta\hat{R}_{1i}^{(B)} \sin\hat{\theta}_{1i}^{(B)} + \Delta\hat{\theta}_{1i}^{(B)} \cdot \hat{R}_{1i}^{(B)} \cos\hat{\theta}_{1i}^{(B)}. \tag{3}$$

Please note that the positioning error is achieved by expanding (2) using Taylor series and ignoring higher order terms. Range error $(\Delta\hat{R}_{1i}^{(B)})$ and angle error $(\Delta\hat{\theta}_{1i}^{(B)})$ are two independent zero mean Gaussian random variables; hence, they are jointly Gaussian. Accordingly, $\Delta\hat{x}_{1i}^{(B)}$ and $\Delta\hat{y}_{1i}^{(B)}$ are jointly Gaussian random variables. The corresponding positioning variances in the main rectangular coordinates are [21]

$$\sigma^2_{\hat{x}_{1i}^{(B)}} = \frac{\sigma_R^2 \cos^2\theta_{1i}^{(B,t)}}{2} + \frac{\sigma_\theta^2 (R_{1i}^{(B,t)})^2 \sin^2\theta_{1i}^{(B,t)}}{2},$$
$$\sigma^2_{\hat{y}_{1i}^{(B)}} = \frac{\sigma_R^2 \sin^2\theta_{1i}^{(B,t)}}{2} + \frac{\sigma_\theta^2 (R_{1i}^{(B,t)})^2 \cos^2\theta_{1i}^{(B,t)}}{2}. \tag{4}$$

Here, $(R_{1i}^{(B,t)}, \theta_{1i}^{(B,t)})$ is the base-node i's true position in the main polar coordinates. So far, we have completed computing nonreference base-nodes' position in the main rectangular coordinates and the corresponding positioning variances.

2.3.2. Target-nodes position estimation fusion

Base-node i estimates target-node j's position as $(\hat{x}_{ij}^{(T)}, \hat{y}_{ij}^{(T)})$ in its own rectangular coordinates, which corresponds to

$$\hat{x}_{ij}^{(T)} = R_{ij}^{(T)} \cos\theta_{ij}^{(T)}, \qquad \hat{y}_{ij}^{(T)} = R_{ij}^{(T)} \sin\theta_{ij}^{(T)}. \tag{5}$$

Here, $(R_{ij}^{(T)}, \theta_{ij}^{(T)})$ is the target-node j's position in base-node i's local polar coordinates estimated by base-node i. The corresponding positioning error is

$$\begin{aligned}\Delta\hat{x}_{ij}^{(T)} &= \Delta R_{ij}^{(T)} \cos\theta_{ij}^{(T)} - \Delta\theta_{ij}^{(T)} \cdot R_{ij}^{(T)} \sin\theta_{ij}^{(T)},\\ \Delta\hat{y}_{ij}^{(T)} &= \Delta R_{ij}^{(T)} \sin\theta_{ij}^{(T)} + \Delta\theta_{ij}^{(T)} \cdot R_{ij}^{(T)} \cos\theta_{ij}^{(T)}.\end{aligned} \tag{6}$$

Similar to the explanation on (3), in (6), $\Delta\hat{x}_{ij}^{(T)}$ and $\Delta\hat{y}_{ij}^{(T)}$ are jointly Gaussian and the corresponding variances are $\sigma^2_{\hat{x}_{ij}^{(T)}}$ and $\sigma^2_{\hat{y}_{ij}^{(T)}}$. Because range and angle estimation errors ($\Delta R_{ij}^{(T)}$ and $\Delta\theta_{ij}^{(T)}$) are independent and zero mean, using (6), it can be shown that

$$\begin{aligned}\sigma^2_{\hat{x}_{ij}^{(T)}} &= E\left(\left(\Delta\hat{x}_{ij}^{(T)}\right)^2\right) = \sigma_R^2 \cos^2\theta_{ij}^{(T,t)} + \sigma_\theta^2 \left(R_{ij}^{(T,t)}\right)^2 \sin^2\theta_{ij}^{(T,t)},\\ \sigma^2_{\hat{y}_{ij}^{(T)}} &= E\left(\left(\Delta\hat{y}_{ij}^{(T)}\right)^2\right) = \sigma_R^2 \sin^2\theta_{ij}^{(T,t)} + \sigma_\theta^2 \left(R_{ij}^{(T,t)}\right)^2 \cos^2\theta_{ij}^{(T,t)}.\end{aligned} \tag{7}$$

In (7), $(R_{ij}^{(T,t)}, \theta_{ij}^{(T,t)})$ is the target-node j's true position in the base-node i's local polar coordinates. When we transform target-node j's position $(\hat{x}_{ij}^{(T)}, \hat{y}_{ij}^{(T)})$ into the main rectangular coordinates, we achieve $(\hat{x}_{1ij}^{(T)}, \hat{y}_{1ij}^{(T)})$

$$\hat{x}_{1ij}^{(T)} = \hat{x}_{1i}^{(B)} + \hat{x}_{ij}^{(T)}, \qquad \hat{y}_{1ij}^{(T)} = \hat{y}_{1i}^{(B)} + \hat{y}_{ij}^{(T)}. \tag{8}$$

The error $(\Delta\hat{x}_{1ij}^{(T)}, \Delta\hat{y}_{1ij}^{(T)})$ and error variance $(\sigma^2_{\hat{x}_{1ij}^{(T)}}, \sigma^2_{\hat{y}_{1ij}^{(T)}})$ in the main coordinates, respectively, correspond to

$$\Delta\hat{x}_{1ij}^{(T)} = \Delta\hat{x}_{1i}^{(B)} + \Delta\hat{x}_{ij}^{(T)}, \qquad \Delta\hat{y}_{1ij}^{(T)} = \Delta\hat{y}_{1i}^{(B)} + \Delta\hat{y}_{ij}^{(T)}, \tag{9}$$

$$\sigma^2_{\hat{x}_{1ij}^{(T)}} = \sigma^2_{\hat{x}_{1i}^{(B)}} + \sigma^2_{\hat{x}_{ij}^{(T)}}, \qquad \sigma^2_{\hat{y}_{1ij}^{(T)}} = \sigma^2_{\hat{y}_{1i}^{(B)}} + \sigma^2_{\hat{y}_{ij}^{(T)}}. \tag{10}$$

The target-node j's position estimation fusion is implemented via weighted sum across multiple base-nodes

$$\hat{x}_j^{(T)} = \sum_{i=1}^{n} p_{ij} \hat{x}_{1ij}^{(T)}, \qquad \hat{y}_j^{(T)} = \sum_{i=1}^{n} q_{ij} \hat{y}_{1ij}^{(T)}. \tag{11}$$

Here, p_{ij} and q_{ij}, $i = 1, 2, \ldots, n$, are fusion weights for target-node j's x and y coordinates, respectively. Based on (11), in the target-node localization fusion process, the reference base-node provides one-hop positioning information and nonreference base-nodes provide two-hop positioning information. In the fusion, the weight of one-hop positioning (p_{1j}) is larger than that of the two-hop positioning. Accordingly, involving the reference base-node reduces the target-nodes positioning error in the reference base-node coordinates.

The estimation error via the fusion corresponds to

$$\Delta\hat{x}_j^{(T)} = \sum_{i=1}^{n} p_{ij} \cdot \Delta\hat{x}_{1ij}^{(T)}, \qquad \Delta\hat{y}_j^{(T)} = \sum_{i=1}^{n} q_{ij} \cdot \Delta\hat{y}_{1ij}^{(T)}. \tag{12}$$

Now, because, as explained for (3) and (6), $\Delta\hat{x}_{1ij}^{(T)}$ and $\Delta\hat{y}_{1ij}^{(T)}$ are jointly Gaussian random variables, their linear combinations that are $\Delta\hat{x}_j^{(T)}$ and $\Delta\hat{y}_j^{(T)}$ would be jointly Gaussian as well. The fusion objective function is the minimization of the mean square of the positioning circular error ($\Delta r_j = \sqrt{\Delta\hat{x}_j^{(T)^2} + \Delta\hat{y}_j^{(T)^2}}$)

$$(p_{1j}, \ldots, p_{nj}, q_{1j}, \ldots, q_{nj}) = \underset{\text{s.t. } \sum_{i=1}^{n} p_{ij}=1,\ \sum_{i=1}^{n} q_{ij}=1}{\arg\min} E(\Delta r_j^2). \tag{13}$$

Lagrange multipliers are used to solve (13), and the fusion weights for target-node j's position estimation are [21]

$$p_{ij} = \frac{1/\sigma^2_{\hat{x}_{1ij}^{(T)}}}{\sum_{k=1}^{n} 1/\sigma^2_{\hat{x}_{1kj}^{(T)}}}, \qquad q_{ij} = \frac{1/\sigma^2_{\hat{y}_{1ij}^{(T)}}}{\sum_{k=1}^{n} 1/\sigma^2_{\hat{y}_{1kj}^{(T)}}}. \tag{14}$$

In the theoretical fusion weights' calculation (14), the real nodes' position is used. However, in real application, we use the measured value in place of the real value, and its impact is evaluated via simulation. With these fusion weights, the fused target-node j's positioning error variance $(\sigma^2_{\hat{x}_j^{(T)}}, \sigma^2_{\hat{y}_j^{(T)}})$ is calculated as follows:

$$\sigma^2_{\hat{x}_j^{(T)}} = \sum_{i=1}^{n} p_{ij}^2 \cdot \sigma^2_{\hat{x}_{1ij}^{(T)}}, \qquad \sigma^2_{\hat{y}_j^{(T)}} = \sum_{i=1}^{n} q_{ij}^2 \cdot \sigma^2_{\hat{y}_{1ij}^{(T)}}. \tag{15}$$

And the corresponding mean square of the positioning circular error is

$$E(\Delta r_j^2) = \frac{1}{\sum_{i=1}^{n} \left(1/\sigma^2_{\hat{x}_{1ij}^{(T)}}\right)} + \frac{1}{\sum_{i=1}^{n} \left(1/\sigma^2_{\hat{y}_{1ij}^{(T)}}\right)}. \tag{16}$$

2.4. Shortcoming of semidistributed multinode TOA-DOA fusion

The semidistributed multinode TOA-DOA fusion localization technique suffers from coordinate transformation. Target-nodes' position should be transformed from base-nodes local coordinates to the reference base-node coordinates (the main coordinates) prior to the fusion. If a target-node is not localized by the reference base-node via any hop, then the target-node position estimated by any base-node cannot be transformed to the main coordinates. In this case, the target-node cannot be localized in the main coordinates, even if it is localized by multiple base-nodes.

Another condition is that a target-node is localized by multiple base-nodes; the reference base-node can localize some of the base-nodes but not all of them via any hop. In this case, the base-nodes that are not localized by the reference base-nodes would not contribute in the target-node position estimation fusion although the position of the target-node can be estimated through other base-nodes.

The third condition is that a target-node is localized by multiple base-nodes via multiple hops in the main coordinates. In this case, due to the coordinates' transformation, the positioning error increases with the number of localization hops. Thus, the positioning performance would highly drop.

3. CEP OF THE SEMIDISTRIBUTED MULTINODE TOA-DOA FUSION

CEP of the target-node position estimation by the semidistributed multinode TOA-DOA fusion with any given base-nodes and target-node geometrical distribution corresponds to

$$\mathrm{CEP}_{\mathrm{point}} = P_{\mathrm{point}}(\Delta r_j \le \beta\sigma_R) = \int_0^{\beta\sigma_R} f_{\mathrm{point},\Delta r_j}(\Delta r_j)\, d\Delta r_j. \tag{17}$$

Here, β is a nonnegative number that normalizes the positioning error with respect to σ_R. Δr_j is the target-node j's position estimation circular error with given nodes' geometrical distribution (the relative position of base-nodes and target-node); and, $f_{\mathrm{point},\Delta r_j}(\Delta r_j)$ is the circular error probability density function (PDF) with the given nodes geometrical distribution. In MANETs, all nodes are moving; hence, nodes' geometrical distribution is continuously changing. We can achieve infinite possible geometrical distribution as there are infinite *points* in an area. In (17), we use the subscript "point" to represent a possible node geometrical distribution in MANETs. The circular error PDF changes with the variations in the base-nodes and target-node geometrical distribution. Now, in order to find the CEP, the PDF of $\Delta r_j[f_{\mathrm{point},\Delta r_j}(\Delta r_j)]$ should be first determined. Recall that $\Delta r_j = \sqrt{\Delta\hat{x}_j^{(T)^2} + \Delta\hat{y}_j^{(T)^2}}$; hence, we should first find the joint PDF of $\Delta\hat{x}_j^{(T)}$ and $\Delta\hat{y}_j^{(T)}$, that is, $f_{\Delta\hat{x}_j^{(T)},\Delta\hat{y}_j^{(T)}}(\Delta\hat{x}_j^{(T)}, \Delta\hat{y}_j^{(T)})$. The covariance matrix of $\Delta\hat{x}_j^{(T)}$ and $\Delta\hat{y}_j^{(T)}$ corresponds to

$$\Lambda = \begin{bmatrix} \Lambda_{11} & \Lambda_{12} \\ \Lambda_{21} & \Lambda_{22} \end{bmatrix} = \begin{bmatrix} \sigma^2_{\hat{x}_j^{(T)}} & \rho\sigma_{\hat{x}_j^{(T)}}\sigma_{\hat{y}_j^{(T)}} \\ \rho\sigma_{\hat{x}_j^{(T)}}\sigma_{\hat{y}_j^{(T)}} & \sigma^2_{\hat{y}_j^{(T)}} \end{bmatrix}. \tag{18}$$

The fused target-node j's positioning error variances $(\sigma^2_{\hat{x}_j^{(T)}}, \sigma^2_{\hat{y}_j^{(T)}})$ were calculated in Section 2, and the covariance of $\Delta\hat{x}_j^{(T)}$ and $\Delta\hat{y}_j^{(T)}$ is calculated in Appendix B. In addition, in Section 2, we have shown that $\Delta\hat{x}_j^{(T)}$ and $\Delta\hat{y}_j^{(T)}$ are jointly Gaussian. Hence, the joint PDF of $\Delta\hat{x}_j^{(T)}$ and $\Delta\hat{y}_j^{(T)}$ corresponds to [34, Section 2.1, Equation 150]

$$f_{\Delta\hat{x}_j^{(T)},\Delta\hat{y}_j^{(T)}}(\Delta\hat{x}_j^{(T)}, \Delta\hat{y}_j^{(T)}) = \frac{1}{2\pi|\Lambda|^{0.5}} \exp\left(-\frac{1}{2}\left[\Delta\hat{x}_j^{(T)} \quad \Delta\hat{y}_j^{(T)}\right]\Lambda^{-1}\left[\Delta\hat{x}_j^{(T)} \quad \Delta\hat{y}_j^{(T)}\right]^T\right). \tag{19}$$

Here, $|\cdot|$ refers to the matrix determinant calculation. Recall that $\Delta r_j = \sqrt{\Delta\hat{x}_j^{(T)^2} + \Delta\hat{y}_j^{(T)^2}}$; thus, the CDF of Δr_j would correspond to (C.1) (see Appendix C). According to the details presented in Appendix C, the point PDF of Δr_j corresponds to

$$f_{\mathrm{point},\Delta r_j}(\Delta r_j) = \frac{\Delta r_j}{|\Lambda|^{0.5}} \exp\left(\frac{\Lambda_{11}+\Lambda_{22}}{-4|\Lambda|}\Delta r_j^2\right) \cdot I_0\left(\frac{\Delta r_j^2\sqrt{(\Lambda_{22}-\Lambda_{11})^2 + \Lambda_{12}^2}}{4|\Lambda|}\right). \tag{20}$$

Incorporating (20) into (17), we can calculate the CEP (point CEP) of the target-node position estimation for any given base-nodes and target-node geometrical distribution, which corresponds to

$$\mathrm{CEP}_{\mathrm{point}} = \int_0^{\beta\sigma_R} \frac{\Delta r_j}{|\Lambda|^{0.5}} \exp\left(\frac{\Lambda_{11}+\Lambda_{22}}{-4|\Lambda|}\Delta r_j^2\right) \cdot I_0\left(\frac{\Delta r_j^2\sqrt{(\Lambda_{22}-\Lambda_{11})^2 + \Lambda_{12}^2}}{4|\Lambda|}\right) d\Delta r_j. \tag{21}$$

There is no theoretical solution for the integration of (21); hence, we evaluate it numerically and compare the numerical result with the simulation result. The average CEP is achieved by averaging the point CEP in (21) over all possible base-nodes and target-node geometrical distribution (i.e., all possible point CEPs) in the MANET.

4. CEP OF GPS-AIDED TOA (DOA) FUSION

Here, first we derive the relationship of the total range (angle) estimation error and the range (angle) errors generated due to two factors: base-nodes range (angle) estimations and GPS positioning errors (Section 4.1). In the next step, we derive the relationship of the base-nodes total range (angle) estimation errors and the target-node positioning errors projected on x and y axes (Section 4.2). Finally, using the relationship derived in Section 4.2, we derive the positioning CEP for GPS-aided TOA (DOA) fusion.

4.1. The impact of GPS positioning error on the final TOA (DOA) estimation

Figure 2 shows the structure of the MANET that applies GPS-aided TOA (DOA) fusion to localize target-nodes. Here, we assume TOA/range (DOA/angle) estimation errors are independent zero mean Gaussian random variables. In these two localization methods, the position of base-node i [$(x_i^{(B,t)}, y_i^{(B,t)})$, $i = 1, 2, \ldots, n$, and n is the number of base-nodes in the MANET] is estimated using GPS receiver as follows:

$$x_i^{(B,t)} = x_{G,i}^{(B)} + \Delta x_{G,i}^{(B)}, \qquad y_i^{(B,t)} = y_{G,i}^{(B)} + \Delta y_{G,i}^{(B)}. \tag{22}$$

In (22), $(x_{G,i}^{(B)}, y_{G,i}^{(B)})$ is base-node i's position estimated by GPS receiver, and it is known; and, $(\Delta x_{G,i}^{(B)}, \Delta y_{G,i}^{(B)})$ is the

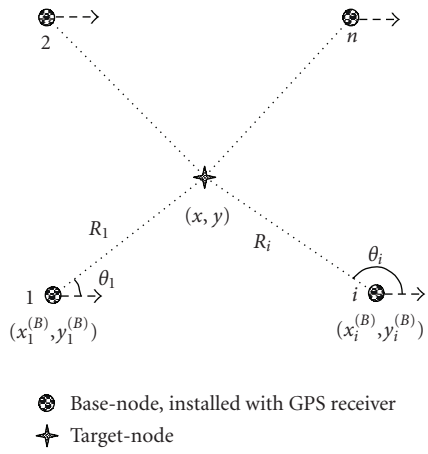

Figure 2: The structure of the MANET that applies GPS-aided TOA (DOA) fusion.

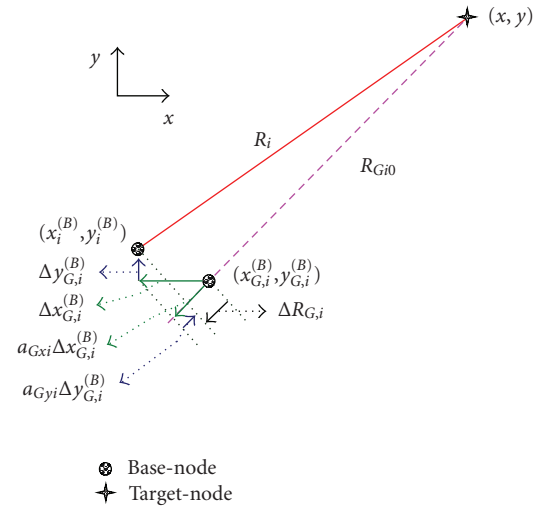

Figure 3: Transformation of GPS positioning error to range estimation error.

positioning error. The range and angle from the target-node with assumed known position (x,y) to base-node i are, respectively, represented by

$$\begin{aligned} R_i &= f_{G,i}\left(x_i^{(B,t)}, y_i^{(B,t)}\right) \\ &= \sqrt{\left(x_i^{(B,t)} - x\right)^2 + \left(y_i^{(B,t)} - y\right)^2} \\ &= \sqrt{\left(x_{G,i}^{(B)} + \Delta x_{G,i}^{(B)} - x\right)^2 + \left(y_{G,i}^{(B)} + \Delta y_{G,i}^{(B)} - y\right)^2}, \end{aligned} \tag{23}$$

$$\begin{aligned} \theta_i &= g_{G,i}\left(x_i^{(B,t)}, y_i^{(B,t)}\right) \\ &= \tan^{-1}\left(\frac{y_i^{(B,t)} - y}{x_i^{(B,t)} - x}\right) \\ &= \tan^{-1}\left(\frac{y_{G,i}^{(B)} + \Delta y_{G,i}^{(B)} - y}{x_{G,i}^{(B)} + \Delta x_{G,i}^{(B)} - x}\right). \end{aligned} \tag{24}$$

Here, the subscript G,i indicates that the data is achieved via GPS receiver for the base-node i. Let

$$\begin{aligned} R_{Gi0} &= \sqrt{\left(x_{G,i}^{(B)} - x\right)^2 + \left(y_{G,i}^{(B)} - y\right)^2}, \\ a_{Gxi} &= \frac{\partial f_{G,i}\left(x_{G,i}^{(B)}, y_{G,i}^{(B)}\right)}{\partial x_{G,i}^{(B)}}, \\ a_{Gyi} &= \frac{\partial f_{G,i}\left(x_{G,i}^{(B)}, y_{G,i}^{(B)}\right)}{\partial y_{G,i}^{(B)}}, \\ b_{Gxi} &= \frac{\partial g_{G,i}\left(x_{G,i}^{(B)}, y_{G,i}^{(B)}\right)}{\partial x_{G,i}^{(B)}}, \\ b_{Gyi} &= \frac{\partial g_{G,i}\left(x_{G,i}^{(B)}, y_{G,i}^{(B)}\right)}{\partial y_{G,i}^{(B)}}. \end{aligned} \tag{25}$$

Applying Taylor series to expand (23) and (24), and ignoring higher order terms, the range estimation error $(\Delta R_{G,i})$ and angle estimation error $(\Delta\theta_{G,i})$ generated by the GPS positioning error are derived as follows:

$$\begin{aligned} \Delta R_{G,i} &= f_{G,i}\left(x_i^{(B)}, y_i^{(B)}\right) - f_{G,i}\left(x_{G,i}^{(B)}, y_{G,i}^{(B)}\right) \\ &= a_{Gxi}\cdot\Delta x_{G,i}^{(B)} + a_{Gyi}\cdot\Delta y_{G,i}^{(B)}, \\ \Delta\theta_{G,i} &= g_{G,i}\left(x_i^{(B)}, y_i^{(B)}\right) - g_{G,i}\left(x_{G,i}^{(B)}, y_{G,i}^{(B)}\right) \\ &= b_{Gxi}\cdot\Delta x_{G,i}^{(B)} + b_{Gyi}\cdot\Delta y_{G,i}^{(B)}. \end{aligned} \tag{26}$$

Based on [28], $\Delta x_{G,i}^{(B)}$ and $\Delta y_{G,i}^{(B)}$ are zero mean jointly Gaussian random variables with the same variances σ_G^2; in addition, GPS receivers perform independently; hence, $\Delta R_{G,i}$ $(\Delta\theta_{G,i})$, $i = 1,2,\ldots,n$ are independent zero mean Gaussian random variables. The variances of $\Delta R_{G,i}$ and $\Delta\theta_{G,i}$ correspond to

$$\sigma_{R_{G,i}}^2 = E\left[\left(a_{Gxi}\cdot\Delta x_{G,i}^{(B)} + a_{Gyi}\cdot\Delta y_{G,i}^{(B)}\right)^2\right] = \sigma_G^2, \tag{27}$$

$$\sigma_{\theta_{G,i}}^2 = E\left[\left(b_{Gxi}\cdot\Delta x_{G,i}^{(B)} + b_{Gyi}\cdot\Delta y_{G,i}^{(B)}\right)^2\right] = \frac{\sigma_G^2}{R_{Gi0}^2}. \tag{28}$$

Here, a_{Gxi} and a_{Gyi} are the direction cosines of the unit vector pointing from target-node to the base-node i's position estimated by GPS with respect to x and y axes, respectively (see Figure 3). Because base-nodes and GPS receivers perform independently, in GPS-aided TOA fusion, two independent sources of errors can be defined: base-nodes range estimation error (ΔR_i) and the range estimation error $(\Delta R_{G,i})$ generated by the GPS positioning error.

Now, when the GPS positioning error is very small with respect to the distance between base-node i and target-node, the line connecting the calculated position of the base-node to the target-node (pink line in Figure 3) and the line connecting the true position of the base-node to target-node (red line in Figure 3) would approximately overlap. In this case, the range error generated by the GPS positioning error $(\Delta R_{G,i})$ can be projected on the line connecting target-node

to the true position of the base-node as well. In addition, the base-node range estimation error (ΔR_i) is in the direction from target-node to base-node.

These two errors can be linearly combined to achieve the total range estimation error ($\Delta R_i'$). Based on the same discussion, we can calculate the total angle estimation error ($\Delta\theta_i'$). The total range and angle estimation errors and their variances, respectively, correspond to

$$\Delta R_i' = \Delta R_i + \Delta R_{G,i}, \qquad \Delta\theta_i' = \Delta\theta_i + \Delta\theta_{G,i}, \tag{29}$$

$$\sigma_{R_i'}^2 = \sigma_R^2 + \sigma_{R_{G,i}}^2, \qquad \sigma_{\theta_i'}^2 = \sigma_\theta^2 + \sigma_{\theta_{G,i}}^2. \tag{30}$$

Here, $\sigma_R^2(\sigma_\theta^2)$ is the base-node range (angle) estimation error variance. Based on (27), (28), and (30), we achieve that $\sigma_{R_i'}^2 = \sigma_{R_j'}^2 = \sigma_{R'}^2$ for any i and j, but $\sigma_{\theta_i'}^2 \neq \sigma_{\theta_j'}^2$, if $i \neq j$.

4.2. GPS-aided TOA (DOA) fusion localization error

In this section, we first introduce the iterative algorithm in TOA (DOA) fusion, and then derive the relationship of the total range (angle) estimation errors, that is, $\Delta R_i'$ ($\Delta\theta_i'$) in (29), and the target-node positioning errors projected on x and y axes.

Consider (x, y) as the unknown true position of the target-node, then the target-node range (R_i) and angle (θ_i) with respect to base-node i are expressed as

$$R_i = f_i(x, y) = \sqrt{\left(x_i^{(B,t)} - x\right)^2 + \left(y_i^{(B,t)} - y\right)^2}, \tag{31}$$

$$\theta_i = g_i(x, y) = \tan^{-1}\left\{\frac{\left(y_i^{(B,t)} - y\right)}{\left(x_i^{(B,t)} - x\right)}\right\}. \tag{32}$$

Here, $(x_i^{(B,t)}, y_i^{(B,t)})$ is base-node i's true position that is known, and $i \in \{1, 2, \ldots, n\}$, n is the number of base-nodes. In TOA fusion, $n \geq 3$; and, in DOA fusion, $n \geq 2$. Please note that (32) has the same structure as (24), however, (24) is used to transform GPS positioning error to angle estimation error (the target-node position (x, y) is assumed known), while (32) is used to transform the total angle estimation error to positioning error (base-node i's true position $(x_i^{(B,t)}, y_i^{(B,t)})$ is assumed known). Equations (31) and (32) are nonlinear equations; hence, we apply iterative algorithm to calculate x and y in (31) and (32) using target-node range (angle) with respect to multiple base-nodes [28]. The algorithm replaces (x, y) in (31) and (32) with an initial guess of target-node position and calculates the associated position error. Then, it updates the initial guess and repeats the process till the error satisfies the accuracy requirement. The algorithm details follow.

Let (x_T, y_T) denote the approximate target-node position in TOA fusion. In the first step, we guess the approximate position (see Section 4.3 below for generating the initial guess). Then, the target-node position is expressed as

$$x = x_T + \Delta x_T, \qquad y = y_T + \Delta y_T. \tag{33}$$

Here, $(\Delta x_T, \Delta y_T)$ denotes the offset of the approximate target-node position from the true position. Using the approximate position (x_T, y_T), the approximate range (R_i'') is calculated as follows:

$$R_i'' = f_i(x_T, y_T) = \sqrt{\left(x_i^{(B,t)} - x_T\right)^2 + \left(y_i^{(B,t)} - y_T\right)^2}. \tag{34}$$

Incorporating (33) in (31), we achieve the following:

$$\begin{aligned} R_i &= f_i(x_T + \Delta x_T, y_T + \Delta y_T) \\ &= \sqrt{\left[x_i^{(B,t)} - (x_T + \Delta x_T)\right]^2 + \left[y_i^{(B,t)} - (y_T + \Delta y_T)\right]^2}. \end{aligned} \tag{35}$$

Expanding (35) using Taylor series about the approximate position and ignoring higher order terms leads to

$$\begin{aligned} R_i &= f_i(x_T + \Delta x_T, y_T + \Delta y_T) \\ &= f_i(x_T, y_T) + \frac{\partial f_i(x_T, y_T)}{\partial x_T}\Delta x_T + \frac{\partial f_i(x_T, y_T)}{\partial y_T}\Delta y_T. \end{aligned} \tag{36}$$

Let

$$h_{xi} = \frac{\partial f_i(x_T, y_T)}{\partial x_T}, \qquad h_{yi} = \frac{\partial f_i(x_T, y_T)}{\partial y_T}. \tag{37}$$

Now, rearranging (36), we achieve the approximated range error as follows:

$$\Delta R_i'' = R_i - R_i'' = h_{xi}\cdot\Delta x_T + h_{yi}\cdot\Delta y_T. \tag{38}$$

Two unknown values Δx_T and Δy_T in (38) can be calculated using range information obtained by multiple ($n > 2$) base-nodes: let

$$\begin{aligned} \mathbf{R} &= \begin{bmatrix} R_1 & \cdots & R_n \end{bmatrix}^T, \\ \mathbf{R}'' &= \begin{bmatrix} R_1'' & \cdots & R_n'' \end{bmatrix}^T, \\ \Delta\mathbf{R}'' &= \mathbf{R} - \mathbf{R}'' = \begin{bmatrix} \Delta R_1'' & \cdots & \Delta R_n'' \end{bmatrix}, \\ \mathbf{H} &= \begin{bmatrix} h_{x1} & \cdots & h_{xn} \\ h_{y1} & \cdots & h_{yn} \end{bmatrix}^T, \\ \mathbf{X} &= \begin{bmatrix} x & y \end{bmatrix}^T, \\ \mathbf{X}_T &= \begin{bmatrix} x_T & y_T \end{bmatrix}^T, \\ \Delta\mathbf{X}_T &= \mathbf{X} - \mathbf{X}_T = \begin{bmatrix} \Delta x_T & \Delta y_T \end{bmatrix}^T, \end{aligned} \tag{39}$$

we have (see [35])

$$\Delta\mathbf{R}'' = \mathbf{H}\cdot\Delta\mathbf{X}_T. \tag{40}$$

The position offset (the positioning error) corresponds to

$$\Delta\mathbf{X}_T = \left(\mathbf{H}^T\mathbf{H}\right)^{-1}\mathbf{H}^T\cdot\Delta\mathbf{R}''. \tag{41}$$

Note that (41) is calculated using the target-node approximate position (x_T, y_T). If the position offset does not

satisfy the positioning accuracy requirement, we can iterate the above process with the updated approximation till the position offset satisfies the accuracy requirement. The approximation is updated by replacing $\mathbf{X}_T$ with $\mathbf{X}_T + \Delta\mathbf{X}_T$, that is,

$$\mathbf{X}_T \longleftarrow \mathbf{X}_T + \Delta\mathbf{X}_T. \tag{42}$$

When the position offset satisfies the accuracy requirement, we localize the target-node at $\mathbf{X}_T$ and achieve the position offset ($\Delta\mathbf{X}_T$).

In GPS-aided TOA fusion, the approximate range error ($\Delta R_i''$) defined in (38) can be modeled as a linear combination of the total range estimation error ($\Delta R_i'$) defined in (29) and a complementary part ($\Delta R_{C,i}$) [28], that is,

$$\Delta R_i'' = \Delta R_i' + \Delta R_{C,i}. \tag{43}$$

Accordingly, the target-node position offset ($\Delta x_T, \Delta y_T$) can be modeled as a linear combination of the position error ($\Delta x_T', \Delta y_T'$) generated by the total range estimation error ($\Delta R_i'$) and the position error ($\Delta x_{C,T}, \Delta y_{C,T}$) generated by the complementary range error ($\Delta R_{C,i}$)

$$\Delta x_T = \Delta x_T' + \Delta x_{C,T}, \qquad \Delta y_T = \Delta y_T' + \Delta y_{C,T}. \tag{44}$$

Let

$$\begin{aligned}
\Delta\mathbf{R}' &= \begin{bmatrix} \Delta R_1' & \cdots & \Delta R_n' \end{bmatrix}^T, \\
\Delta\mathbf{R}_C &= \begin{bmatrix} \Delta R_{C,1} & \cdots & \Delta R_{C,n} \end{bmatrix}^T, \\
\Delta\mathbf{X}_T' &= \begin{bmatrix} \Delta x_T' & \Delta y_T' \end{bmatrix}^T, \\
\Delta\mathbf{X}_{C,T} &= \begin{bmatrix} \Delta x_{C,T} & \Delta y_{C,T} \end{bmatrix}^T,
\end{aligned} \tag{45}$$

in the matrix form, we have

$$\Delta\mathbf{R}'' = \Delta\mathbf{R}' + \Delta\mathbf{R}_C, \qquad \Delta\mathbf{X}_T = \Delta\mathbf{X}_T' + \Delta\mathbf{X}_{C,T}, \tag{46}$$

where $\Delta\mathbf{X}_T'$ is generated by the total range estimation error ($\Delta\mathbf{R}'$), and it cannot be diminished in the iteration process. While $\Delta\mathbf{R}_C$ and $\Delta\mathbf{X}_{C,T}$ are generated by the arithmetic and diminished in the iteration process. At the end of the iteration, $\Delta\mathbf{X}_{C,T}$ and $\Delta\mathbf{R}_C$ are small and can be ignored. In other words, the final positioning error is a function of GPS precision and the base-node range estimation accuracy. Incorporating (46) in (41) and ignoring $\Delta\mathbf{X}_{C,T}$ and $\Delta\mathbf{R}_C$, the positioning error in GPS-aided TOA fusion corresponds to

$$\Delta\mathbf{X}_T' = (\mathbf{H}^T\mathbf{H})^{-1}\mathbf{H}^T \cdot \Delta\mathbf{R}'. \tag{47}$$

In DOA fusion, using the same iteration method presented above, we can estimate the target-node position with the target-node angles with respect to two or more base-nodes. And the target-node position estimation error corresponds to

$$\Delta\mathbf{X}_D' = (\mathbf{B}^T\mathbf{B})^{-1}\mathbf{B}^T \cdot \Delta\boldsymbol{\theta}'. \tag{48}$$

In (48), $\Delta\mathbf{X}_D' = \mathbf{X} - \mathbf{X}_D = [\Delta x_D' \;\; \Delta y_D']^T$ is the target-node position error generated by the total angle estimation error, $\mathbf{X}_D = [x_D \;\; y_D]^T$ is the estimated target-node position via the iteration method,

$$\begin{aligned}
\mathbf{B} &= \begin{bmatrix} b_{x1} & \cdots & b_{xn} \\ b_{y1} & \cdots & b_{yn} \end{bmatrix}^T, \\
b_{xi} &= \frac{\partial g_i(x_D, y_D)}{\partial x_D}, \\
b_{yi} &= \frac{\partial g_i(x_D, y_D)}{\partial y_D}, \\
\Delta\boldsymbol{\theta}' &= \begin{bmatrix} \Delta\theta_1' & \cdots & \Delta\theta_n' \end{bmatrix}^T
\end{aligned} \tag{49}$$

is the total angle estimation error.

4.3. Initialization of the iteration process

The initial guess that leads to the convergence of the iteration process should support the following properties. For GPS-aided TOA fusion, first, the determinant of the matrix $\mathbf{H}^T\mathbf{H}$ ($\mathbf{H}$ has been defined in (39) should not be zero (i.e., $|\mathbf{H}^T\mathbf{H}| \neq 0$). If $|\mathbf{H}^T\mathbf{H}| = 0$, $(\mathbf{H}^T\mathbf{H})^{-1}$ would not exist, and we cannot continue the iteration to estimate the target-node position. Hence, in each iteration step, we calculate $|\mathbf{H}^T\mathbf{H}|$. If the initial guess makes $|\mathbf{H}^T\mathbf{H}|$ equal zero or very small, we should ignore this initial guess and try a new initial guess to restart the iteration process.

Second, the approximate target-node position circular error ($\sqrt{\Delta x_T^2 + \Delta y_T^2}$) should converge to a small value as the iteration process continues. In the iteration process, if the approximate target-node position circular error in each step is not obviously smaller than that in the previous step, the iteration would diverse. Hence, in each iteration step, we calculate the ratio of the circular error of the new step to the previous one. If this ratio is considerably less than one, we keep the initial guess; else, we ignore that and try a new one.

Similarly, in GPS-aided DOA fusion, we monitor the determinant of $\mathbf{B}^T\mathbf{B}$ ($|\mathbf{B}^T\mathbf{B}|$) ($\mathbf{B}$ was defined in (48)), and the target-node position circular error ($\sqrt{\Delta x_D^2 + \Delta y_D^2}$) to guarantee the validity of the initial guess.

4.4. CEP of GPS-aided TOA (DOA) fusion

In Section 4.1, we showed that $\Delta R_i'$, $i = 1, 2, \ldots, n$ are zero mean Gaussian random variables with the same variance. In addition, base-nodes perform independently and GPS receivers perform independently; hence, $\Delta R_i'$, $i = 1, 2, \ldots, n$, are independent and identically distributed zero mean Gaussian random variables. Positioning errors $\Delta x_T'$ and $\Delta y_T'$ are linear combinations of $\Delta R_i'$, $i = 1, 2, \ldots, n$; hence, $\Delta x_T'$ and $\Delta y_T'$ are jointly Gaussian random variables. Based on similar analysis, in GPS-aided DOA fusion, positioning

errors Δx_D and Δy_D would also be jointly Gaussian random variables. Let

$$\mathbf{V} = \begin{bmatrix} V_{11} & V_{12} \\ V_{21} & V_{22} \end{bmatrix} = \mathrm{cov}(\Delta \mathbf{X}'_T),$$
$$\mathbf{U} = \begin{bmatrix} U_{11} & U_{12} \\ U_{21} & U_{22} \end{bmatrix} = \mathrm{cov}(\Delta \mathbf{X}'_D), \tag{50}$$

and apply the same approach as that of Section 3, the target-node positioning point PDF in the GPS-aided TOA (DOA) fusion is derived as follows:

$$f_{\mathrm{point},\Delta r_T}(\Delta r_T) = \frac{\Delta r_T}{|\mathbf{V}|^{0.5}} \exp\left(\frac{V_{11}+V_{22}}{-4|\mathbf{V}|}\Delta r_T^2\right) \cdot I_0\left(\frac{\Delta r_T^2\sqrt{(V_{22}-V_{11})^2+V_{12}^2}}{4|\mathbf{V}|}\right),$$
$$f_{\mathrm{point},\Delta r_D}(\Delta r_D) = \frac{\Delta r_D}{|\mathbf{U}|^{0.5}} \exp\left(\frac{U_{11}+U_{22}}{-4|\mathbf{U}|}\Delta r_D^2\right) \cdot I_0\left(\frac{\Delta r_D^2\sqrt{(U_{22}-U_{11})^2+U_{12}^2}}{4|\mathbf{U}|}\right). \tag{51}$$

Here, $\Delta r_T = \sqrt{\Delta x_T'^2 + \Delta y_T'^2}$ ($\Delta r_D = \sqrt{\Delta x_D'^2 + \Delta y_D'^2}$) is the GPS-aided TOA (DOA) fusion positioning circular error with a given nodes' geometrical distribution. Incorporating (51) into (17), the point CEP of GPS-aided TOA fusion and GPS-aided DOA fusion are derived as follows:

$$\mathrm{CEP}_{\mathrm{point},T} = \int_0^{\beta\sigma_R} \frac{\Delta r_T}{|\mathbf{V}|^{0.5}} \exp\left(\frac{V_{11}+V_{22}}{-4|\mathbf{V}|}\Delta r_T^2\right) \cdot I_0\left(\frac{\Delta r_T^2\sqrt{(V_{22}-V_{11})^2+V_{12}^2}}{4|\mathbf{V}|}\right) d\Delta r_T, \tag{52}$$

$$\mathrm{CEP}_{\mathrm{point},D} = \int_0^{\beta\sigma_\theta R s} \frac{\Delta r_D}{|\mathbf{U}|^{0.5}} \exp\left(\frac{U_{11}+U_{22}}{-4|\mathbf{U}|}\Delta r_D^2\right) \cdot I_0\left(\frac{\Delta r_D^2\sqrt{(U_{22}-U_{11})^2+U_{12}^2}}{4|\mathbf{U}|}\right) d\Delta r_D. \tag{53}$$

In (53), we select $R_s = \sigma_R/\sigma_\theta$ for the convenience of comparing GPS-aided DOA fusion and the other two techniques. Averaging the point CEP achieved in (52) and (53) over all possible nodes' geometrical distribution in the MANET, we achieve the average CEP of the MANET.

5. SIMULATIONS AND DISCUSSIONS

In this part, (1) we compare the probability of target-nodes being localized in the three localization techniques with respect to the MANET coverage radius in the condition that the MANET coverage area radius is greater than half of the base-node coverage radius; (2) verify the theoretically computed point CEP and compare the average localization CEP of the three localization methods in the condition that the MANET coverage area radius is smaller or equal to the half of the base-node coverage radius; (3) we consider the same nodes' geometrical distribution for the two comparisons. In addition, we compare the average localization CEP with respect to different parameters. These parameters include the number of base-nodes in the MANET, the MANET coverage radius, DOA estimation error standard deviation, and the ratio of GPS positioning error variance on x (y) axis, σ_G^2, to the base-node range estimation error variance, σ_R^2, that is $Z = \sigma_G^2/\sigma_R^2$.

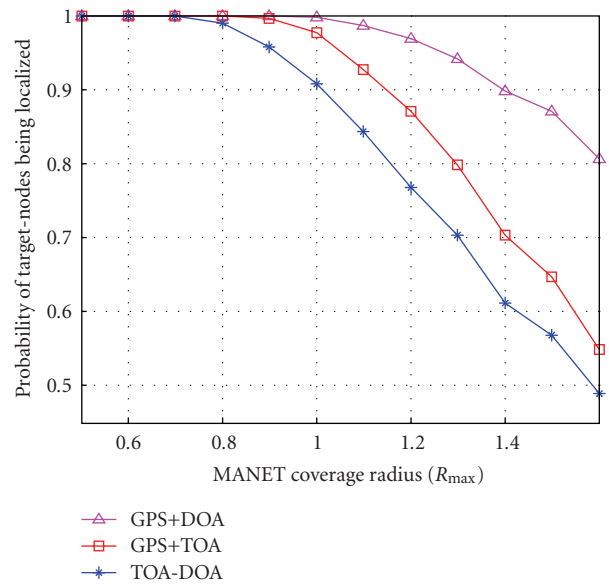

Figure 4: Comparison of probability of target-nodes being localized with respect to MANET coverage radius, with 5 base-nodes in the MANET.

It should be noted that only in GPS-available environments, we can apply GPS-aided TOA (DOA) fusion to localize target-nodes; while the semidistributed multinode TOA-DOA fusion localization technique is not affected by the availability of GPS service.

5.1. Simulation assumptions

In order to make a fair comparison across all techniques, we assume that (1) all nodes are uniformly distributed in the MANET; (2) the nodes geometrical distribution for these three localization techniques is the same; (3) in GPS-aided TOA (DOA) fusion, base-nodes' position is determined via GPS receivers; (4) for the first simulation (Figure 4), the MANET coverage radius is $\alpha R_{\max}$, $0.5 < \alpha \leq 1.6$, there are 5 base-nodes in the MANET, and the performance is evaluated in terms of the probability of target-node being localized; (5) for other simulations, the MANET coverage radius is $\alpha R_{\max}$, $0 < \alpha \leq 0.5$, that is, all base-nodes can estimate other nodes' TOA and (or) DOA in the MANET, and the localization performance is evaluated in terms of average positioning CEP $[P(\Delta r \leq \beta\sigma_R)]$ as a function of β.

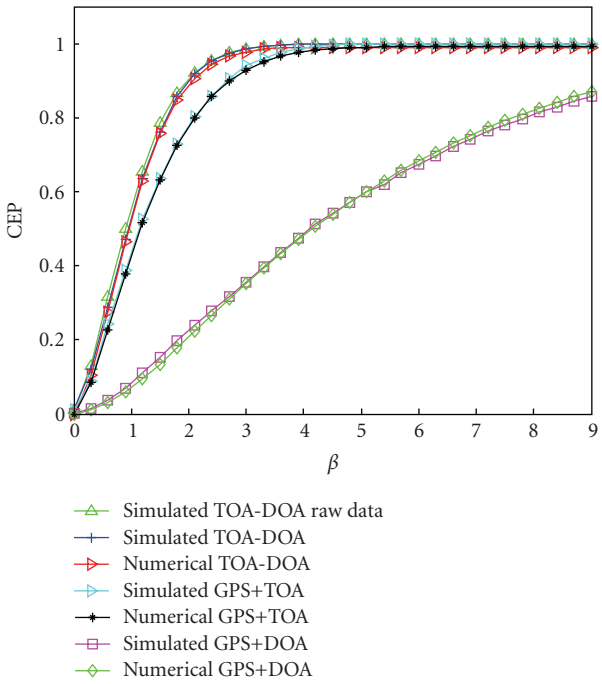

Figure 5: Numerical and simulated point CEP with 5 base-nodes, $R_{\max} = 80\sigma_R$, $\sigma_\theta = 2^\circ$, and the ratio $Z = 0.5$.

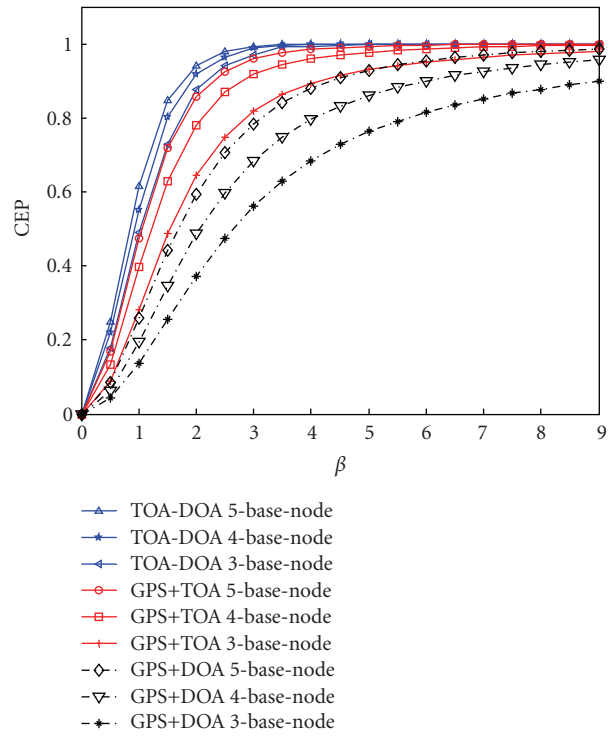

Figure 6: Average CEP comparison versus base-nodes number with $R_{\max} = 80\sigma_R$, $\sigma_\theta = 2^\circ$, and the ratio $Z = 0.5$.

5.2. Simulation results

(1) *Probability of target-nodes being localized comparison:* here, we calculate the probability of target-nodes being localized in MANETs with a radius larger than half of the base-nodes coverage radius ($0.5R_{\max}$). Figure 4 depicts the following: (1) as the MANET coverage radius increases from $0.5R_{\max}$ to $1.6R_{\max}$, the probability of target-nodes being localized decreases from 1 to about 0.8 (for GPS-aided DOA fusion), 0.55 (for GPS-aided TOA fusion), and 0.49 (for semidistributed multinode TOA-DOA fusion); (2) with the same MANETs coverage radius, the probability of target-nodes being localized in the semidistributed method is always lower than the other two methods.

(2) *Point CEP verification:* here, we generate the numerical results of point CEP for three localization techniques and compare them to the corresponding simulation results. Figure 5 shows the following: (1) the simulation results are consistent with the numerical results; (2) there is a very small gap between the simulation and numerical results because we ignored higher order terms in the computation of the positioning error; (3) the positioning CEP of the multinode TOA-DOA fusion with raw estimations is consistent with that simulated CEP using true values; (4) the positioning CEP of GPS-aided DOA fusion is much lower than that of the other two methods. Note that the point CEP only represents the system performance at a known (but randomly selected) nodes geometrical distribution. Thus, it might be better or worse than the average CEP. The average CEP is generated over a large number of point CEPs.

(3) *Average CEP:* here, we compare the average CEP of the three localization techniques considering four parameters: the number of base-nodes in the MANET, MANET coverage radius, DOA estimation standard deviation, and $Z = \sigma_G^2/\sigma_R^2$. The results are shown in Figures 6, 7, 8, and 9. These figures show (1) all methods perform better as the number of base-nodes increases; (2) the performance of GPS-aided TOA fusion is independent of MANET coverage radius, but the performance of other two techniques decreases as the MANET coverage radius increases; (3) the performance of the semidistributed multinode TOA-DOA fusion and GPS-aided DOA fusion decreases as the DOA estimation error increases; (4) as the ratio $Z = \sigma_G^2/\sigma_R^2$ increases, the performance of GPS-aided TOA fusion and GPS-aided DOA fusion decreases, while the semidistributed multinode TOA-DOA fusion is not affected by GPS performance; (5) considering $R_{\max} = 80\sigma_R$, $\sigma_\theta = 1^\circ$ or 2°, and $Z = \sigma_G^2/\sigma_R^2 \geq 0.5$, semidistributed multinode TOA-DOA fusion performs the best and GPS-aided DOA fusion performs the worst.

5.3. Discussions

The semidistributed multinode TOA-DOA fusion localization technique takes the advantages of the base-nodes' property, the capability of localizing other nodes independently; hence, it does not depend on GPS to localize base-node in MANETs. Accordingly, it is applicable in GPS-denied environments as well.

As discussed in Section 2.4, the semidistributed fusion method suffers from the coordinate transformation. The probability of target-nodes being not localized by the reference base-node via any hop increases as the MANET

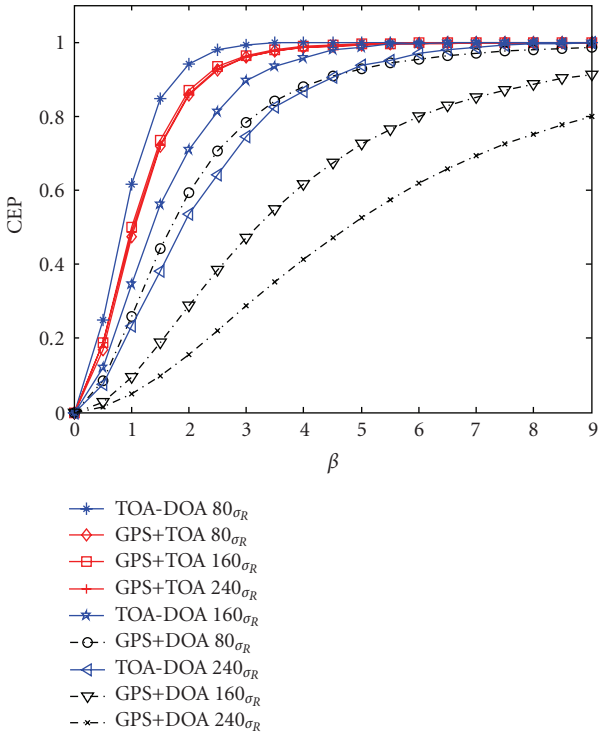

Figure 7: Average CEP comparison versus MANET radius with 5 base-nodes, $\sigma_\theta = 2^\circ$, and the ratio $Z = 0.5$.

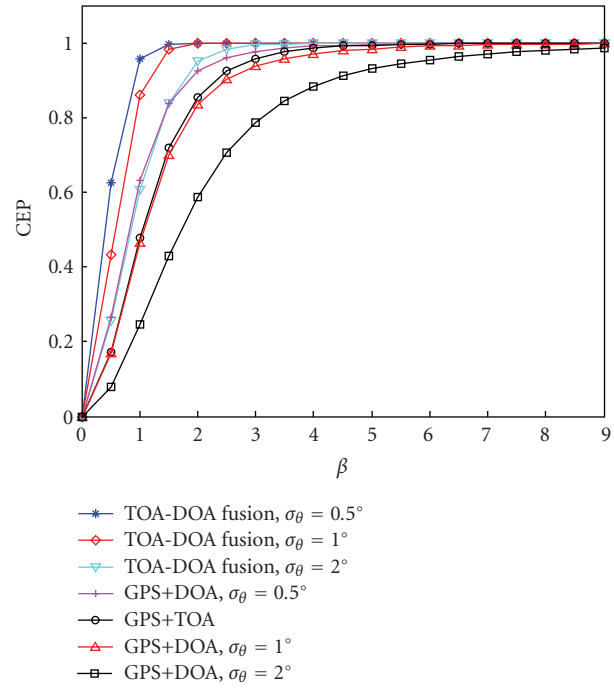

Figure 8: Average CEP comparison versus DOA estimation error with 5 base-nodes, $R_{\max} = 80\sigma_R$, $\sigma_\theta = 2^\circ$, and the ratio $Z = 0.5$.

coverage radius increases from half of base-node coverage radius. In this case, the probability of target-nodes that are not localized in the main coordinates increases. But GPS-aided TOA and DOA fusion methods do not suffer from coordinate transformation. In these two methods, all base-nodes and target-nodes are localized in earth-centered earth-fixed (ECEF) Cartesian coordinates; hence, no coordinates' transformation is needed. In any MANET scale, as long as a target-node's TOA (DOA) is estimated by at least 3 (2) base-nodes, it would be localized in the ECEF Cartesian coordinates. Finally, because GPS-aided DOA fusion technique needs only two base-nodes for localization, it is less vulnerable to coverage radius compared to GPS-aided TOA fusion.

The positioning error generated by DOA estimation increases as the target-node and base-node distance increases; however, the positioning error generated by TOA estimation remains unchanged. Hence, the average positioning performance of the semidistributed technique would be high (low) in a moderate (large) scale MANET.

The GPS-aided DOA fusion error is high. The reason is explained as follows. In the GPS-aided DOA fusion, the total DOA estimation error is due to two factors: base-node DOA estimation error and DOA estimation error generated by GPS positioning error. When the base-node and target-node distance is low, the DOA estimation error generated by GPS would be high and it leads to a high positioning error. In addition, when the base-node and target-node distance is high, the base-node DOA estimation error would be dominant, which also translated to a high positioning error due to high distance.

In GPS-aided TOA fusion, the TOA estimation error includes base-node TOA estimation error and TOA estimation error generated by GPS positioning error. These two errors are independent of the distance between base-node and target-node. Hence, average GPS-aided TOA fusion performance is independent of the MANET scale as long as all base-nodes can localize all target-nodes.

The semidistributed multinode TOA-DOA fusion can be applied to MANETs in GPS denied environments. In the GPS available environments and all base-nodes localize all target-nodes, the semidistributed localization method is suitable for moderate scale MANETs and GPS-aided TOA fusion is suitable for large scale MANETs. Finally, it should be noted that the performance evaluation discussed here would be applicable to the centralized scheme, if the centralized scheme applies the same reference base-node selection method used in the semidistributed scheme.

For simplicity, we assumed TOA and DOA estimation errors are independent and have identical zero mean Gaussian distributions. However, in general, TOA and DOA estimation errors are functions of many variables including signal-to-noise ratio (SNR), bandwidth, channel multipath effects, and the availability of LOS [36, 37]. When LOS signal is available and it is stronger than NLOS signal, (a) TOA estimation errors can be considered zero mean Gaussian random variables with their variance normalized with respect to the target-node and base-node distance (as distance increases, TOA estimation error variance increases) [38]; and, (b) the PDF of DOA estimation error fits Laplacian

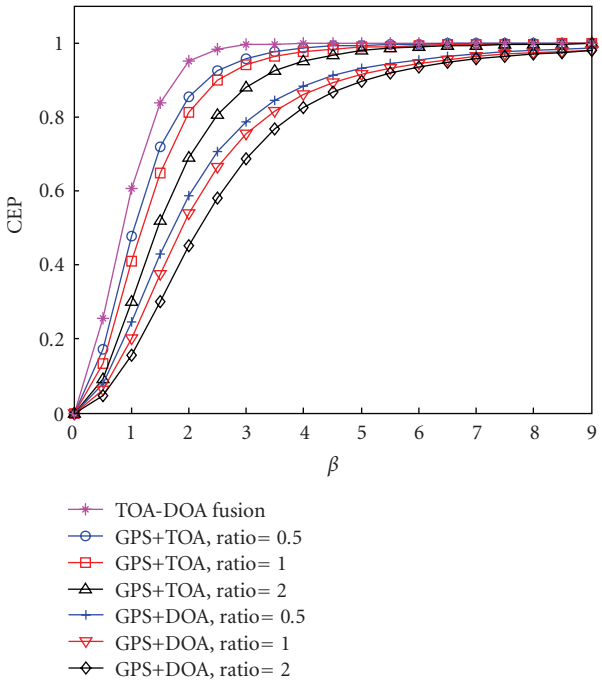

FIGURE 9: Average CEP comparison versus different ratio Z with 5 base-nodes, $R_{\max} = 80\sigma_R$, and $\sigma_\theta = 2^\circ$.

distribution [39]. Whereas in the scenario that LOS is not available or LOS and NLOS signal power are comparable, the statistics of TOA and DOA estimation errors are complicated and hard to compute [40]. In addition, depending on the nature of channels, the TOA and DOA estimation errors might become independent [39] or correlated [41].

If the PDF of the TOA and DOA estimation errors are not identical, the joint distribution of $\Delta\hat{x}_j^{(T)}$ and $\Delta\hat{y}_j^{(T)}$ would be hard to compute (in the scenario that the PDF of TOA and DOA estimation errors are identical zero mean Gaussian, we use (19) to calculate the joint PDF of $\Delta\hat{x}_j^{(T)}$ and $\Delta\hat{y}_j^{(T)}$). Accordingly, the fusion CEP would be difficult to evaluate. Thus, making any conclusion would not be plausible.

The performance of the semidistributed multinode TOA-DOA fusion is altered by the variances of the positioning error over x and y axes defined in (10), which depends on base-nodes localization variance (calculated in (4)) and target-node localization variance (calculated in (7)). If DOA and TOA estimation errors are correlated, then an additional term, that is, a function of their correlation coefficient would appear in (4) and (7). This additional term ultimately degrades the performance of the fusion in the proposed semidistributed technique.

The other two techniques, that is, GPS-aided TOA fusion and GPS-aided DOA fusion only need the estimation of TOA or DOA. Therefore, in the first review, one may deduce that the performance of GPS-aided TOA fusion and GPS-aided DOA fusion may not be altered by the correlation of TOA and DOA estimation errors. But, let us see what may impact (or increase) the correlation of TOA and DOA estimation errors. We predict that multipath environment may impact (or increase) the correlation of TOA and DOA estimation errors. Why? Because the estimation performance of TOA and DOA reduces as the channel multipath effect increases. Thus, higher correlation might be translated into lower performance of GPS-aided TOA fusion and GPS-aided DOA fusion as well. Accordingly, it is hard to make a solid conclusion when comparing our technique with GPS-aided TOA fusion and GPS-aided DOA fusion when TOA and DOA estimation errors are considered correlated. This subject may need a separate fundamental investigation.

6. CONCLUSIONS

In this paper, we theoretically derive and compare the point CEP of the semidistributed multinode TOA-DOA fusion, GPS-aided TOA fusion, and GPS-aided DOA fusion localization techniques. In addition, we verify the results via simulation, and compare the average CEP of these three localization techniques under the same nodes' geometrical distribution, and the same estimation error variance.

Simulation results confirm that the semidistributed multinode TOA-DOA fusion localization technique is not suitable for MANETs with radius larger than half of base-nodes coverage radius. In the condition of MANET coverage radius smaller than or equal to half of base-nodes coverage radius, the semidistributed multinode TOA-DOA fusion localization technique leads to a better performance in moderate scale MANETs. GPS-aided TOA fusion localization technique leads to a better performance in large scale MANETs. Finally, GPS-aided DOA fusion leads to a lower performance compared to the other two techniques.

APPENDICES

A. REFERENCE BASE-NODE SELECTION

Two techniques are proposed for base-node selection. The first approach is optimal, but needs high computational cost. The second approach is suboptimal. It needs lower computational cost while its performance is very close to the optimal technique.

The optimal reference base-node selection minimizes the average mean square positioning circular error of the MANET. The selection method follows (a) let $i = 1$; (b) assume base-node i is the reference base-node, localize non-reference base-nodes, and cluster the MANET; (c) localize all m target-nodes in the main coordinates, and generate average mean square positioning circular error for this selection $(1/m)\sum_{j=1}^{m} E(\Delta r_{j,i}^2)$ using (16); (d) if $i < n$, replace i with $i + 1$ and go to step (b); (e) select the base-node, v, with the minimized average mean square positioning circular error as the reference base-node as follows:

$$v_{\text{optimal}} = \arg\min_i \frac{1}{m}\sum_{j=1}^{m} E(\Delta r_{j,i}^2). \tag{A.1}$$

In the optimal method, all target-nodes are localized n times via data fusion, this leads to high time and power consumption. To reduce the power and time consumption,

we apply a suboptimal selection scheme. Considering (10) and (16), the upper bound of $\sum_{j=1}^{m} E(\Delta r_{j,i}^2)$ corresponds to

$$\begin{aligned}\sum_{j=1}^{m} E(\Delta r_{j,i}^2) &= \sum_{j=1}^{m}\left(\frac{1}{\sum_{k=1}^{n}\left(1/\sigma_{\hat{x}_{ikj}^{(T)}}^2\right)}+\frac{1}{\sum_{k=1}^{n}\left(1/\sigma_{\hat{y}_{ikj}^{(T)}}^2\right)}\right)\\ &< \sum_{j=1}^{m}\left[\min_k\left(\sigma_{\hat{x}_{ikj}^{(T)}}^2\right)+\min_k\left(\sigma_{\hat{y}_{ikj}^{(T)}}^2\right)\right]\\ &\le \sum_{j=1}^{m}\left(\sigma_{x_{iij}}^2+\sigma_{y_{iij}}^2\right)\\ &= \sum_{j=1}^{m}\left(\sigma_R^2+\sigma_\theta^2\left(R_{ij}^{(T,t)}\right)^2\right).\end{aligned} \tag{A.2}$$

Here, $R_{ij}^{(T,t)}$ is the true distance between base-node i and target-node j. σ_R^2 and σ_θ^2 are constants; hence, the optimal selection technique of (A.1) can be replaced by the suboptimal technique that follows

$$v_{\text{sub-optimal}} = \arg\min_i \sum_{j=1}^{m}\left(R_{ij}^{(T,t)}\right)^2. \tag{A.3}$$

In the suboptimal reference-node selection method, the distance from base-nodes to target-nodes is measured once, and only distance square summation is calculated n times. This highly reduces the computation cost and complexity. In addition, using this method, time and power would be saved.

B. CROSS-CORRELATION CALCULATION

The covariance of $\Delta\hat{x}_j^{(T)}$ and $\Delta\hat{y}_j^{(T)}$ corresponds to

$$\rho\sigma_{\hat{x}_j^{(T)}}\sigma_{\hat{y}_j^{(T)}} = E\left(\Delta\hat{x}_j^{(T)}\cdot\Delta\hat{y}_j^{(T)}\right). \tag{B.1}$$

Incorporating (12) in (B.1) leads to

$$\rho\sigma_{\hat{x}_j^{(T)}}\sigma_{\hat{y}_j^{(T)}} = \sum_{i=1}^{n} p_{ij}q_{ij}E\left(\Delta\hat{x}_{1ij}^{(T)}\cdot\Delta\hat{y}_{1ij}^{(T)}\right). \tag{B.2}$$

In (B.2), if $i = 1$, the target-node j's positioning information is provided by the reference base-node and the error is one-hop positioning error, which does not include the coordinate transformation error. Accordingly, in (9), $\Delta\hat{x}_{1i}^{(B)} = 0$ and $\Delta\hat{y}_{1i}^{(B)} = 0$. Now, incorporating the results of (6) in (9), the one-hop positioning error covariance corresponds to

$$E\left(\Delta\hat{x}_{11j}^{(T)}\cdot\Delta\hat{y}_{11j}^{(T)}\right) = \left(\sigma_R^2-\sigma_\theta^2 R_{1j}^{(T,t)^2}\right)\sin\theta_{1j}^{(T,t)}\cos\theta_{1j}^{(T,t)}. \tag{B.3}$$

And, if $i \neq 1$, the target-node j's positioning information is provided by nonreference base-node and the error is two-hop positioning error, which includes the coordinate transformation error. Considering (3), (6), and (9), the two-hop positioning error covariance would correspond to

$$\begin{aligned}E\left(\Delta\hat{x}_{1ij}^{(T)}\cdot\Delta\hat{y}_{1ij}^{(T)}\right) &= \left(\sigma_R^2-\sigma_\theta^2 R_{1i}^{(B,t)^2}\right)\sin\theta_{1i}^{(B,t)}\cos\theta_{1i}^{(B,t)}\\ &\quad+\left(\sigma_R^2-\sigma_\theta^2 R_{ij}^{(T,t)^2}\right)\sin\theta_{ij}^{(T,t)}\cos\theta_{ij}^{(T,t)}.\end{aligned} \tag{B.4}$$

Incorporating (B.3) and (B.4) in (B.2), we can calculate the covariance of $\Delta\hat{x}_j^{(T)}$ and $\Delta\hat{y}_j^{(T)}$, and we can achieve

$$\rho\sigma_{\hat{x}_j^{(T)}}\sigma_{\hat{y}_j^{(T)}} \neq 0. \tag{B.5}$$

Hence, $\Delta\hat{x}_j^{(T)}$ and $\Delta\hat{y}_j^{(T)}$ are not independent.

C. POINT PDF DERIVATION

In (12), $\Delta\hat{x}_j^{(T)}$ and $\Delta\hat{y}_j^{(T)}$ are jointly Gaussian, and $\Delta r_j = \sqrt{\Delta\hat{x}_j^{(T)^2}+\Delta\hat{y}_j^{(T)^2}}$; hence, the CDF of Δr_j corresponds to

$$\begin{aligned}&F_{\text{point},\Delta r_j}(\Delta r_j)\\ &\quad=\int_{-\Delta r_j}^{\Delta r_j}\left[\int_{-\mathcal{X}}^{\mathcal{X}} f_{\Delta\hat{x}_j^{(T)},\Delta\hat{y}_j^{(T)}}\left(\Delta\hat{x}_j^{(T)},\Delta\hat{y}_j^{(T)}\right)d\Delta\hat{x}_j^{(T)}\right]d\Delta\hat{y}_j^{(T)},\end{aligned} \tag{C.1}$$

where $\mathcal{X}$ denotes $\sqrt{\Delta r_j^2-\Delta\hat{y}_j^{(T)^2}}$.

Differentiating the CDF with respect to Δr_j leads to the PDF of Δr_j as follows:

$$\begin{aligned}&f_{\text{point},\Delta r_j}(\Delta r_j)\\ &\quad=\int_{-\Delta r_j}^{\Delta r_j}\frac{\Delta r_j}{\sqrt{\Delta r_j^2-\Delta y_j^2}}\\ &\qquad\times\left[f_{\Delta\hat{x}_j^{(T)},\Delta\hat{y}_j^{(T)}}\left(\sqrt{\Delta r_j^2-\Delta\hat{y}_j^{(T)^2}},\Delta\hat{y}_j^{(T)}\right)\right.\\ &\qquad\left.+f_{\Delta\hat{x}_j^{(T)},\Delta\hat{y}_j^{(T)}}\left(-\sqrt{\Delta r_j^2-\Delta\hat{y}_j^{(T)^2}},\Delta\hat{y}_j^{(T)}\right)\right]d\Delta\hat{y}_j^{(T)}.\end{aligned} \tag{C.2}$$

Let $\Delta\hat{y}_j^{(T)} = \Delta r_j\cdot\sin\phi$, then $\sqrt{\Delta r_j^2-\Delta\hat{y}_j^{(T)^2}} = \Delta r_j\cdot\cos\phi$, $d\Delta y_j = \Delta r_j\cdot\cos\phi\cdot d\phi$, $\phi\in[-\pi/2,\pi/2]$. Accordingly, (C.2) leads to

$$\begin{aligned}&f_{\text{point},\Delta r_j}(\Delta r_j)\\ &\quad=\int_{-\pi/2}^{\pi/2}\Delta r_j\left[f_{\Delta\hat{x}_j^{(T)},\Delta\hat{y}_j^{(T)}}\left(\Delta r_j\cos\phi,\Delta r_j\sin\phi\right)\right.\\ &\qquad\left.+f_{\Delta\hat{x}_j^{(T)},\Delta\hat{y}_j^{(T)}}\left(-\Delta r_j\cos\phi,\Delta r_j\sin\phi\right)\right]d\phi.\end{aligned} \tag{C.3}$$

Incorporating (19) into (C.3), we have

$$\begin{aligned}&f_{\text{point},\Delta r_j}(\Delta r_j)\\ &\quad=\frac{\Delta r_j}{2\pi|\Lambda|^{0.5}}\times\int_{-\pi/2}^{\pi/2}\left[\exp\left(\frac{\sigma_{\hat{y}_j^{(T)}}^2\cos^2\phi-\mathcal{Q}}{-2|\Lambda|}\Delta r_j^2\right)\right.\\ &\qquad\left.+\exp\left(\frac{\sigma_{\hat{y}_j^{(T)}}^2\cos^2\phi+\mathcal{Q}}{-2|\Lambda|}\Delta r_j^2\right)\right]d\phi,\end{aligned} \tag{C.4}$$

where $\mathcal{Q}$ denotes $\rho\sigma_{\hat{x}_j^{(T)}}\sigma_{\hat{y}_j^{(T)}}\sin 2\phi+\sigma_{\hat{x}_j^{(T)}}^2\sin^2\phi$.

Because, $2\cos^2\phi = 1 + \cos 2\phi$, and $2\sin^2\phi = 1 - \cos 2\phi$, (B.5) corresponds to

$$f_{\text{point},\Delta r_j}(\Delta r_j) = \frac{\Delta r_j}{2\pi|\Lambda|^{0.5}} \exp\left(\frac{\sigma^2_{\hat{y}_j^{(T)}} + \sigma^2_{\hat{x}_j^{(T)}}}{-4|\Lambda|}\Delta r_j^2\right) \times \int_{-\pi/2}^{\pi/2}\left[\exp\left(\frac{\mathcal{W} - 2\rho\sigma_{\hat{x}_j^{(T)}}\sigma_{\hat{y}_j^{(T)}}\sin 2\phi}{-4|\Lambda|}\Delta r_j^2\right) + \exp\left(\frac{\mathcal{W} + 2\rho\sigma_{\hat{x}_j^{(T)}}\sigma_{\hat{y}_j^{(T)}}\sin 2\phi}{-4|\Lambda|}\Delta r_j^2\right)\right]d\phi, \tag{C.5}$$

where $\mathcal{W}$ denotes $(\sigma^2_{\hat{y}_j^{(T)}} - \sigma^2_{\hat{x}_j^{(T)}})\cos 2\phi$.

Let $A = (\Delta r_j/|\Lambda|^{0.5})\exp(((\sigma^2_{\hat{y}_j^{(T)}} + \sigma^2_{\hat{x}_j^{(T)}})/-4|\Lambda|)\Delta r_j^2)$, $B = \sigma^2_{\hat{y}_j^{(T)}} - \sigma^2_{\hat{x}_j^{(T)}}$, $C = 2\rho\sigma_{\hat{x}_j^{(T)}}\sigma_{\hat{y}_j^{(T)}}$, $\gamma = \Delta r_j^2\sqrt{B^2 + C^2}/4|\Lambda|$, $\cos\beta = B/\sqrt{B^2 + C^2}$, and $\alpha = 2\phi$, then $d\phi = 1/2d\alpha$, $\alpha \in [-\pi, \pi]$. Incorporating these parameters, (C.5) would be equal to

$$f_{\text{point},\Delta r_j}(\Delta r_j) = \frac{A}{4\pi}\int_{-\pi}^{\pi}\{\exp[-\gamma\cdot\cos(\alpha+\beta)] + \exp[-\gamma\cdot\cos(\alpha-\beta)]\}d\alpha. \tag{C.6}$$

Here, $g(\alpha) = \exp(-\gamma\cdot\cos(\alpha))$ is an even periodic function with period of 2π. Hence, (C.6) is simplified to

$$\begin{aligned} f_{\text{point},\Delta r_j}(\Delta r_j) &= \frac{A}{\pi}\cdot\int_0^{\pi}\exp(-\gamma\cdot\cos\alpha)d\alpha \\ &= \frac{A}{\pi}\cdot\int_0^{\pi}\exp(\gamma\cdot\cos\alpha)d\alpha \\ &= A\cdot I_0(\gamma). \end{aligned} \tag{C.7}$$

In (C.7), $I_0(\gamma) = 1/\pi\int_0^{\pi}e^{\gamma\cos\phi}d\phi$ is the modified Bessel function of the first kind and zero order. In addition,

$$\begin{aligned} A &= \frac{\Delta r_j}{|\Lambda|^{0.5}}\exp\left(\frac{\sigma^2_{\hat{y}_j^{(T)}} + \sigma^2_{\hat{x}_j^{(T)}}}{-4|\Lambda|}\Delta r_j^2\right) \\ &= \frac{\Delta r_j}{|\Lambda|^{0.5}}\exp\left(\frac{\Lambda_{11} + \Lambda_{22}}{-4|\Lambda|}\Delta r_j^2\right), \\ \gamma &= \frac{\Delta r_j^2\sqrt{B^2 + C^2}}{4|\Lambda|} = \frac{\Delta r_j^2\sqrt{(\Lambda_{22} - \Lambda_{11})^2 + \Lambda_{12}^2}}{4|\Lambda|}. \end{aligned} \tag{C.8}$$

Hence,

$$f_{\text{point},\Delta r_j}(\Delta r_j) = \frac{\Delta r_j}{|\Lambda|^{0.5}}\exp\left(\frac{\Lambda_{11}+\Lambda_{22}}{-4|\Lambda|}\Delta r_j^2\right)\cdot I_0\left(\frac{\Delta r_j^2\sqrt{(\Lambda_{22}-\Lambda_{11})^2+\Lambda_{12}^2}}{4|\Lambda|}\right). \tag{C.9}$$

REFERENCES

[1] K. Amouris, "Position-based broadcast TDMA scheduling for mobile ad-hoc networks (MANETS) with advantaged nodes," in *Proceedings of IEEE Military Communications Conference (MILCOM '05)*, vol. 1, pp. 252–257, Atlatnic City, NJ, USA, October 2005.

[2] E. C. Haddad, C. Despins, and P. Mermelstein, "Capacity gain of zone division for a position-based resource allocation algorithm in WCDMA uplink data transmission," in *Proceedings of the 14th IEEE on Personal, Indoor and Mobile Radio Communications (PIMRC '03)*, vol. 1, pp. 597–601, Beijing, China, September 2003.

[3] V. Sumathy, P. Narayanasmy, K. Baskaran, and T. Purusothaman, "GLS with secure routing in ad-hoc networks," in *Proceedings of the Conference on Convergent Technologies for Asia-Pacific Region (TENCON '03)*, vol. 3, pp. 1072–1076, Bangalore, India, October 2003.

[4] S. M. M. Rahman, M. Mambo, A. Inomata, and E. Okamoto, "An anonymous on-demand position-based routing in mobile ad hoc networks," in *Proceedings of International Symposium on Applications and the Internet (SAINT '06)*, pp. 300–306, Phoenix, Ariz, USA, January 2006.

[5] J. Xie and L. Huang, "Specification and verification of position based routing for mobile ad hoc system," in *Proceedings of the 5th International Conference on Computer and Information Technology (CIT '05)*, pp. 406–409, Shanghai, China, September 2005.

[6] N. Bulusu, J. Heidemann, and D. Estrin, "GPS-less low-cost outdoor localization for very small devices," *IEEE Personal Communications*, vol. 7, no. 5, pp. 28–34, 2000.

[7] Y. Shang, W. Ruml, Y. Zhang, and M. P. J. Fromherz, "Localization from mere connectivity," in *Proceedings of the 4th International Symposium on Mobile Ad Hoc Networking and Computing (MobiHoc '03)*, pp. 201–212, Annapolis, Md, USA, June 2003.

[8] L. Hu and D. Evans, "Localization for mobile sensor networks," in *Proceedings of the 10th Annual International Conference on Mobile Computing and Networking (MOBICOM '04)*, pp. 45–57, Philadelphia, Pa, USA, September 2004.

[9] S. Zhou and J. K. Pollard, "Position measurement using Bluetooth," *IEEE Transactions on Consumer Electronics*, vol. 52, no. 2, pp. 555–558, 2006.

[10] T. Locher, R. Wattenhofer, and A. Zollinger, "Received-signal-strength-based logical positioning resilient to signal fluctuation," in *Proceedings of the 6th International Conference on Software Engineering, Artificial Intelligence, Networking and Parallel/Distributed Computing and 1st ACIS International Workshop on Self-Assembling Wireless Networks (SNPD/SAWN '05)*, pp. 396–402, Towson, Md, USA, May 2005.

[11] H. Karimi and P. Krishnamurthy, "Real-time routing in mobile networks using GPS and GIS techniques," in *Proceedings of the 34th Annual Hawaii International Conference*, p. 255, Maui, Hawaii, USA, January 2001.

[12] A. Boukerche and S. Rogers, "GPS query optimization in mobile and wireless networks," in *Proceedings of the 6th IEEE Symposium on Computers and Communications (ISCC '01)*, pp. 198–203, Hammamet, Tunisia, July 2001.

[13] M. A. Spirito and A. G. Mattioli, "On the hyperbolic positioning of GSM mobile stations," in *Proceedings of the URSI International Symposium on Signals, Systems, and Electronics (ISSSE '98)*, pp. 173–177, Pisa, Italy, September-October 1998.

[14] K. C. Ho and Y. T. Chan, "Solution and performance analysis of geolocation by TDOA," *IEEE Transactions on Aerospace and Electronic Systems*, vol. 29, no. 4, pp. 1311–1322, 1993.

[15] S. S. Ghidary, T. Tani, T. Takamori, and M. Hattori, "A new home robot positioning system (HRPS) using IR switched multi ultrasonic sensors," in *Proceedings of the IEEE International Conference on Systems, Man, and Cybernetics (SMC '99)*, vol. 4, pp. 737–741, Tokyo, Japan, October 1999.

[16] J.-M. Lee, D. H. Lee, H. An, N. Huh, M. K. Kim, and M. H. Lee, "Ultrasonic satellite system for the positioning of mobile robots," in *Proceedings of the 30th Annual Conference of IEEE Industrial Electronics Society (IECON '04)*, vol. 1, pp. 448–453, Busan, Korea, November 2004.

[17] D. Niculescu and B. Nath, "Ad hoc positioning system (APS) using AOA," in *Proceedings of the 22nd Annual Joint Conference of the IEEE Computer and Communications Societies (INFOCOM '03)*, vol. 3, pp. 1734–1743, San Francisco, Calif, USA, March-April 2003.

[18] S. Sayeef, U. K. Madawala, P. G. Handley, and D. Santoso, "Indoor personnel tracking using infrared beam scanning," in *Proceedings of IEEE Position Location and Navigation Symposium (PLANS '04)*, pp. 698–705, Monterey, Calif, USA, April 2004.

[19] A. N. Bishop, P. N. Pathirana, B. Fidan, B. D. O. Anderson, and G. Mao, "Passive angle measurement based localization consistency via geometric constraints," in *Proceedings of Information, Decision and Control Conference (IDC '07)*, pp. 199–204, Adelaide, Australia, February 2007.

[20] H. Tong and S. A. Zekavat, "A novel wireless local positioning system via a merger of DS-CDMA and beamforming: Probability-of-detection performance analysis under array perturbations," *IEEE Transactions on Vehicular Technology*, vol. 56, no. 3, pp. 1307–1320, 2007.

[21] Z. Wang and S. A. Zekavat, "MANET localization via multinode TOA-DOA optimal fusion," in *Proceedings of IEEE Military Communications Conference (MILCOM '06)*, pp. 1–7, Washington, DC, USA, October 2006.

[22] Y. Qi and H. Kobayashi, "On relation among time delay and signal strength based geolocation methods," in *Proceedings of IEEE Global Telecommunications Conference (GLOBECOM '03)*, vol. 7, pp. 4079–4083, San Francisco, Calif, USA, December 2003.

[23] T.-Y. Chen, C.-C. Chiu, and T.-C. Tu, "Mixing and combining with AOA and TOA for the enhanced accuracy of mobile location," in *Proceedings of the 5th European Personal Mobile Communications Conference (EPMCC '03)*, pp. 276–280, Glasgow, UK, April 2003.

[24] S.-L. Dong, J.-M. Wei, T. Xing, and H.-T. Liu, "Constraint-based fuzzy optimization data fusion for sensor network localization," in *Proceedings of the 2nd International Conference on Semantics Knowledge and Grid (SKG '06)*, p. 59, Guilin, China, November 2006.

[25] A. Brown and J. Nordlie, "Integrated GPS/TOA navigation using a positioning and communication software defined radio," in *Proceedings of IEEE/ION Position, Location, and Navigation Symposium (PLANS '06)*, pp. 147–152, San Diego, Calif, USA, April 2006.

[26] T. Eren, W. Whiteley, and P. N. Belhumeur, "Using angle of arrival (bearing) information in network localization," in *Proceedings of the 45th IEEE Conference on Decision and Control (CDC '06)*, pp. 4676–4681, San Diego, Calif, USA, December 2006.

[27] D.-H. Shin and T.-K. Sung, "Comparisons of error characteristics between TOA and TDOA positioning," *IEEE Transactions on Aerospace and Electronic Systems*, vol. 38, no. 1, pp. 307–311, 2002.

[28] E. D. Kaplan, *Understanding GPS: Principles and Applications*, Telecommunications Library, Artech House, Boston, Mass, USA, 1996.

[29] A. G. Dempster, "Dilution of precision in angle-of-arrival positioning systems," *Electronics Letters*, vol. 42, no. 5, pp. 291–292, 2006.

[30] J. T. Gillis, "Computation of the circular error probability integral," *IEEE Transactions on Aerospace and Electronic Systems*, vol. 27, no. 6, pp. 906–910, 1991.

[31] M. Pourkhaatoun, S. A. Zekavat, and J. Pourrostam, "A novel high resolution ICA-based TOA estimation technique," in *Proceedings of IEEE Radar Conference*, pp. 320–324, Waltham, Mass, USA, April 2007.

[32] S. A. Zekavat, A. Kolbus, X. Yang, Z. Wang, J. Pourrostam, and M. Pourkhaatoon, "A novel implementation of DOA estimation for node localization on software defined radios: achieving high performance with low complexity," in *Proceedings of IEEE International Conference on Signal Processing and Communications (ICSPC '07)*, Dubai, UAE, November 2007.

[33] J. Pourrostam, S. A. Zekavat, and H. Tong, "Novel direction-of-arrival estimation techniques for periodic-sense local positioning systems," in *Proceedings of IEEE Radar Conference*, pp. 568–573, Waltham, Mass, USA, April 2007.

[34] J. G. Proakis, *Digital Communications*, Mcgraw-Hill, New York, NY, USA, 4th edition, 2001.

[35] D. J. Torrieri, "Statistical theory of passive location systems," *IEEE Transactions on Aerospace and Electronic Systems*, vol. 20, no. 2, pp. 183–198, 1984.

[36] S. Gezici, H. Kobayashi, and H. V. Poor, "Non-parametric non-line-of-sight identification," in *Proceedings of the 58th IEEE Vehicular Technology Conference (VTC '03)*, vol. 4, pp. 2544–2548, Orlando, Fla, USA, October 2003.

[37] M. Heidari and K. Pahlavan, "A new statistical model for the behavior of ranging errors in TOA-based indoor localization," in *Proceedings of IEEE Wireless Communications and Networking Conference (WCNC '07)*, pp. 2566–2571, Hong Kong, March 2007.

[38] B. Alavi and K. Pahlavan, "Modeling of the distance error for indoor geolocation," in *Proceedings of IEEE Wireless Communications and Networking Conference (WCNC '03)*, vol. 1, pp. 668–672, New Orleans, La, USA, March 2003.

[39] Q. H. Spencer, B. D. Jeffs, M. A. Jensen, and A. L. Swindlehurst, "Modeling the statistical time and angle of arrival characteristics of an indoor multipath channel," *IEEE Journal on Selected Areas in Communications*, vol. 18, no. 3, pp. 347–360, 2000.

[40] S. Venkatraman and J. Caffery Jr., "Hybrid TOA/AOA techniques for mobile location in non-line-of-sight environments," in *Proceedings of IEEE Wireless Communications and Networking Conference (WCNC '04)*, vol. 1, pp. 274–278, Atlanta, Ga, USA, March 2004.

[41] A. Y. Olenko, K. T. Wong, and E. H.-O. Ng, "Analytically derived TOA-DOA statistics of uplink/downlink wireless multipaths arisen from scatterers on an hollow-disc around the mobile," *IEEE Antennas and Wireless Propagation Letters*, vol. 2, pp. 345–348, 2003.